# Paleoceanographic changes at the northern Tethyan margin during the Cenomanian-Turonian Oceanic Anoxic Event (OAE-2)

**Authors:**

Holger Gebhardt[1)], Oliver Friedrich[2),3)], Bettina Schenk[4)], Lyndsey Fox[5)], Malcolm Hart[5)] and Michael Wagreich[4)]

[1)] Geologische Bundesanstalt, Neulinggasse 38, A-1030 Wien, Austria

[2)] National Oceanography Centre Southampton, University of Southampton, European Way, Southampton SO14 3ZH, UK

[3)] present address: Johann Wolfgang Goethe-Universität, Altenhöferallee 1, D-60438 Frankfurt am Main, Germany

[4)] Universität Wien, Althanstraße 14, A-1090 Wien, Austria

[5)] School of Geography, Earth and Environmental Sciences, University of Plymouth, Drake Circus, Plymouth PL4 8AA, UK

holger.gebhardt@geologie.ac.at, o.friedrich@em.uni-frankfurt.de, schenkb2@univie.ac.at, lyndsey.fox@student.plymouth.ac.uk, M.Hart@plymouth.ac.uk, michael.wagreich@univie.ac.at

Corresponding author: Holger Gebhardt, Tel.: 0043-1-7125674250, Fax: 0043-1-712567456

## Abstract

The late Cenomanian – early Turonian Oceanic Anoxic Event (OAE-2) represents major paleoceanographic and faunal perturbations. Samples from the northern Tethyan margin (Rehkogelgraben, Eastern Alps) were investigated in order to trace the paleoceanographic processes. Paleoecologic conditions were reconstructed by combining the results of assemblage counts of indicative microfossil groups (foraminifera, radiolaria). Assemblages, size distributions and abundances show a tripartite subdivision for surface and bottom waters: 1) Oligotrophic surface conditions and oxic bottom waters with a reasonably high food supply for the late Cenomanian interval. 2) An OAE period with black shales characterized by very low numbers but high diversities and a lack of high productivity indicators among planktic foraminifera. Low abundances of small sized benthic foraminifera indicate low oxic-dysoxic conditions at the seafloor. 3) Post-OAE assemblages are characterized by mesotrophic

planktic species and benthic foraminifera suggest oxic bottom waters. It took about 300 ky to re-establish a pelagic carbonate-producing regime. The semi-enclosed basin situation of the Penninic Ocean is thought to be responsible for differences between the high productivity in the world ocean during the OAE-2 and the overall absence of high productivity indicators and high foraminiferal diversities at Rehkogelgraben. The Penninic Ocean may have even served as a refuge during the environmental crisis.

Keywords: Penninic Ocean, Oceanic Anoxic Event 2, foraminifera, radiolaria, trophic levels, oxygenation

## 1. Introduction

The Oceanic Anoxic Event OAE-2 (or Bonarelli Event (Schlanger et al., 1987), or Cenomanian-Turonian Boundary Event, CTBE) is of global significance and has paleoceanographic, paleontologic and sedimentologic (black shale deposition) consequences of economic importance (hydrocarbon source rocks) in the Atlantic Ocean and adjacent seas (e.g., Kuypers et al., 2002; Kolonic et al., 2005). The widespread black shale deposition went along with dysoxic or anoxic conditions extending from deep waters to the photic zone (e.g., Kuypers et al., 2002; Pancost et al., 2004). The mid-Cretaceous, and the late Cenomanian – early Turonian in particular, was a period of global sea-level highstands (e.g., Haq et al., 1987; Sahagian et al., 1996) and $pCO_2$ levels 4 times higher than modern (pre-industrial) values are assumed (e.g., Poulsen et al., 1999, 2001). Turonian sea-surface temperatures were the warmest during the entire Cretaceous-Cenozoic (Wilson et al., 2002). OAE-2 is associated with significant extinction events and faunal turnovers. It influenced the evolution of planktic and benthic foraminifera and many other fossil groups (e.g., Elder, 1989; Kaminski et al., 1999; Premoli Silva and Sliter, 1999; Leckie et al., 2002). The presence of several positive $\delta^{13}C$-excursions during OAE-2 enables the correlation of reference sections from various places (e.g., Tsikos et al., 2004) with the GSSP section at Pueblo, Colorado, USA (e.g., Sageman et al., 2006) and also with the section investigated here (Wagreich et al., 2008). However, the causes of the paleoceanographic changes resulting in different sedimentologic records at various locations are still a matter of debate.

Complete boundary sections around the North Atlantic Ocean show a period (or several episodes) of black shale deposition during the transitional interval from the Cenomanian to the Turonian. This period is usually characterized by high surface productivity, as indicated by several paleontological and geochemical proxies, e.g., dominance of indicative foraminiferal taxa (e.g., Premoli Silva et al., 1999; Coccioni et al., 2006). Our contribution focusses on the paleoceanographic situation during OAE-2 at the northern margin of the Tethys ocean system, in particular the northern margin of the Penninic Ocean (Fig. 1). We combine the results of faunal developments of indicative microfossil groups from planktic (foraminifera, radiolaria) and benthic (foraminifera) habitats. The investigated section in the Rehkogelgraben is the only known described Cenomanian-Turonian boundary section in the Eastern Alps containing a black shale interval. It is therefore a unique opportunity to study the changes in fossil content across the Cenomanian/Turonian boundary and the paleoceanographic development in this part of the early Late Cretaceous world. Sediments of the nearest available oceanic Cenomanian-Turonian boundary sections (Italy, Switzerland) were deposited in different paleogeographic settings (Apulian Block or Briançonnais Domain, i.e., in deeper water-depths). Thus, the Rehkogelgraben section represents the conditions in the Penninic Ocean above carbonate compensation depth, at least at its northern margin. We also compare the foraminiferal record of the Rehkogelgraben with key sections for oceanic and upwelling settings around the North Atlantic Ocean in order to be able to assess the recorded assemblages of the section investigated here. We expect information on the temporal process and the influence of OAE-2 on the oxygenation conditions at the seafloor, productivity indicators, and recovery rates.

The questions addressed in this contribution are: 1) Are there indicators pointing to definable ecologic conditions in the upper and lower mixed layers or greater water depths? 2) What precisely are these conditions? 3) Do these conditions change with time? 4) Can the regional results be easily integrated into already existing paleoceanographic models or is a new concept needed for the Penninic Ocean or the northern Tethyan margin? 5) Was high surface productivity a global phenomenon during OAE-2?

## 2. Geological setting

The present study deals with sediments exposed in the Rehkogelgraben in Upper Austria. The succession of limestones, marls, claystones and black shales is part of the Ultrahelvetic Unit,

outcropping within several tectonic windows in the Rhenodanubian Flysch Zone. The Ultrahelvetic Unit connects the shallow Helvetic shelf in the north and the abyssal Rhenodanubian (Penninic) Flysch basin in the south (Faupl and Wagreich, 2000). Both paleogeographically neighbouring tectonic units are either build up of glauconitic sandstones (Helvetic Unit) or carbonate poor marlstones, shales or turbidites lacking black shales (Rhenodanubian Flysch Zone).

The exact location of the section, geological setting, nannoplankton biostratigraphy, sedimentology and some geochemical parameters have been described in detail by Wagreich et al. (2008, including outcrop photographs). The Rehkogelgraben section (initially described in Kollmann and Summesberger (1982)) comprises exclusively pelagic or hemipelagic sediments. With the exception of one clay layer, no clastic layers (turbidites, contourites, pyroclastites, or bentonites) were found. Three black shale layers were logged and have total organic carbon (TOC) contents of up to 5% (Wagreich et al., 2008). The sediments were deposited in a distal slope environment and overall normal marine salinity can be assumed.

## 3. Material and methods

### 3.1 Sample treatment

We collected 15 marl, calcareous marl, clayey marl and black shale samples to investigate microfossil assemblages and $\delta^{13}C$ ratios of organic matter. These samples were supplemented by five samples collected for an earlier investigation (Wagreich et al., 2008) of the same section. About 60 to 600 g of sediment were disintegrated completely with hydrogen peroxide (1st step) and tenside (Rewoquat W36 90 PG, 2nd step), cleaned with hydrogen peroxide, and washed over a 0.063-mm sieve. The residues were dried and sieved into >0.250, >0.125, and >0.063 mm-fractions to access species distribution in individual size fractions. These fractions were split into manageable subsamples (aliquots) and completely picked for foraminifera (average c. 400 specimens per aliquot for planktic foraminifera) and radiolaria (Tables 1 to 3).

The number of benthic specimens per sample is much less than those for planktic foraminifera. If only the dominant taxa (>5%) are interpreted, Fatela and Taborda (2002) found that 100 specimens were sufficient to obtain reliable results. The interpretations on

benthic foraminifera made here are on taxa with much higher proportions and are therefore considered to be reliable even if the number of specimens picked is lower.

Thin sections were produced from limestones and marly limestones in order to complement the results from disaggregated samples, in particular to support biostratigraphy. Lithology and dry sample weight are listed in Table 4. Microfossil specimens were identified and counted, numbers for individual fractions were recombined according to the split, and abundance (number of specimens per gram dry sediment) was calculated. Radiolaria were picked and counted but were not further classified (Table 3).

Due to the inadequate preservation status of microfossils from the studied section (diagenetic overprint), reliable carbon stable isotope analyses are only possible for bulk rock samples. Thus, we rely on the interpretation of assemblage counts for paleoceanographic reconstructions of the site investigated here and C-isotope analyses are used for stratigraphic purposes only. $\delta^{13}C_{org}$ (Table 4) was measured at the National Oceanographic Center, Southampton, UK, using a GV Instruments Iso-Prime continuous flow mass spectrometer connected to a EuroVector Elemental Analyser. Powdered and decarbonated sediment samples were weighed into tin capsules, inserted in the autosampler and combusted at 1020°C. Analytical results are measured against a laboratory standard and expressed relative to the VPDB standard.

A complete list of all identified taxa is provided in the appendix. Microfossils from sample REH 4/1 from the stratum directly below the thickest black shale layer look extremely abraded. The microfrossils of this sample are therefore considered to be reworked (transported) and are consequently ignored in later interpretations.

## 3.2 Ecological concepts and groups

### 3.2.1 Planktic foraminifera

Reproduction of modern planktic foraminifera usually takes place in the deepest environment during their life cycle or near the thermocline (deep-dwellers, Hemleben et al. (1989)). Comparison with equivalent Cretaceous morphogroups allows for inferences on the habitat of the species investigated here (e.g., Hart and Bailey, 1979; Leckie et al., 1998; West et al.,

1998; Hart, 1999). The assumption of C- and O-isotope incorporation in equilibrium with changes in ambient seawater during subsequent growth stages suggest life cycles similar to modern genera (Norris and Wilson, 1998; Houston et al., 1999). Isotope data from the contributions of Norris and Wilson (1998), Houston et al. (1999), Huber et al. (1999), MacLeod et al. (2000) and Coxall et al. (2007) enable the identification of the occurring morphogroups or genera present. However, isotope data for Cretaceous species are not always unambiguous (e.g., for *Heterohelix*, Huber et al. (1995, 1999), MacLeod et al. (2000), Fassell and Bralower (1999)). Therefore, the successive appearance or disappearance of species or genera along gradients (waterdepth, rise and fall of oxygen minimum zones, nutrient supply) is used to confirm assumed habitats or to find arguments for different ecologic niches (Leckie, 1987; Jarvis et al., 1988; Leary et al., 1989; Koutsoukos and Hart, 1990; Hart, 1999; Premoli Silva and Sliter, 1999). We distinguish between species occupying the upper mixed layer (*Hedbergella* spp., *Gümbelitria cenomana*), the lower mixed layer (intermediate habitats, *Whiteinella* spp.), and deep dwellers from within or below the thermocline (*Rotalipora cushmani, Thalmanninella* spp., *Praeglobotruncana* spp., *Schackoina cenomana*).

Certain species are adapted to eutrophic or unstable conditions (opportunists, *r*-strategists). If such conditions prevail, equilibrium taxa (*K*-strategists) such as *Rotalipora, Thalmanninella* or *Praeglobotruncana* become rare or even disappear from the area (e.g., Jarvis et al., 1988; Leary et al., 1989). *Whiteinella* and *Hedbergella* connect between both groups and are therefore called intermediate species. Dominance of *K*-Strategists is therefore indicative for stable, meso- to highly oligotrophic conditions (Premoli Silva and Sliter, 1999; Coccioni and Luciani, 2004; Friedrich et al., 2008a). Prominent *r*-strategists are *Heterohelix* and *Gümbelitria*. Particularly *Gümbelitria* is known to thrive under conditions where no other planktic foraminifera survive. It is amongst the first to colonize new seaways and has blooms in shallow waters (e.g., Gebhardt, 1997, Leckie et al., 1998), points to nutrient-rich surface waters (Keller et al., 2008) or indicates ecologic disasters (Keller and Pardo, 2004). *Heterohelix* dominates in nearshore assemblages or in unstable areas with salinity or oxygen fluctuations (e.g., Nederbragt, 1991; Nederbragt et al., 1998; Premoli Silva and Sliter, 1999). Also massive productivity disturbances in upwelling areas such as at Tarfaya (Morocco) may lead to strong dominance of heterohelicids (Keller et al., 2008). Therefore, dominance of *Heterohelix* can be seen as a good stress indicator.

Chamber elongation in Cretaceous planktic foraminifera has been interpreted as an adaptive response to eutrophication and corresponding oxygen depletion (e.g., Premoli Silva et al., 1999; Coccioni et al., 2006) because a high surface area to volume ratio enhances gas exchange for metabolic needs (Magniez-Jannin, 1998). Coxall et al. (2007), however, suggest that chamber elongation is an adaptation to a feeding specialization for survival in a food-poor environment close to the OMZ. Prominent schackoinid-rich assemblages frequently characterize the onset and end of OAE-2 in deep-water settings and *Schackoina* is interpreted to be more competitive in low-oxygen, eutrophic waters than other radially elongated chambered forms (Coccioni et al., 2006). Repeated increased abundance of elongated chambered forms in association with some Cretaceous OAEs, Eocene and modern upwelling suggest a close link with episodes of enhanced ocean productivity (Coccioni and Luciani, 2004; Coxall et al., 2007) or extension of the oxygen minimum zone (Friedrich et al., 2008a). *Schackoina* is therefore interpreted as a high-productivity, low oxygen(?) indicator.

### 3.2.2 Benthic foraminifera

Cretaceous species are not found in modern oceans and consequently ecologic interpretations must be made on a generic level for ecologic index taxa or via equivalent morphogroups (e.g., Bernhard, 1986; Koutsoukos and Hart, 1990; Kuhnt and Wiedmann, 1995; West et al., 1998; Gebhardt, 2006). The size distribution of benthic foraminifera can be used to interpret bottom-water oxygenation because small (predominantly deep infaunal) species are assumed to be more adapted to low-oxygen levels of interstitial waters and large organisms demand higher amounts of oxygen for respiration (e.g., Bernhard, 1986; Kaiho, 1994, 1999). Bernhard (1986) distinguished 4 oxic (sphaerical, large planoconvex, biumbilicate, lenticular) and 4 dysoxic (flattened planispiral, cylindrical, tapered, elongated-flattened) morphotypes from Mesozoic and Cenozoic deposits. The detailed study of Koutsoukos and Hart (1990) refined this concept (21 general morphotypes allocated to inferred microhabitats and trophic groups) and applied it to mid-Upper Cretaceous sediments from the Brazilian Sergipe Basin. Kaiho (1994, 1999) developed an oxygenetion index (BFOI) for modern and late Cenozoic environments based on a similar concept. Benthic foraminifera adapted to dysoxic environments frequently follow an opportunistic life strategy and exploit increased food availability. Turrilinids (tapered rounded triserial morphotype of Koutsoukos and Hart (1990)) and small gavelinellids (planoconvex low trochspiral) dominate under such conditions in some Cenomanian to Turonian sediments (Koutsoukos and Hart, 1990; Koutsoukos et al.,

1990; Leckie et al., 1998; West et al., 1998; Gebhardt et al., 2004; Gebhardt, 2006). However, if oxygen is not acting as a limiting factor, food supply largely governs abundance and distribution of species in the sediment (van der Zwaan et al., 1999). In particular the genus *Gabonita* and some species of *Bolivina* (tapered flattened-elongated biserial) have been interpreted to be indicative for increased food supply in combination with high primary production (Kuhnt and Wiedmann, 1995; Holbourn et al., 1999; Gebhardt et al., 2004).

## 4. Stratigraphy

In order to achieve the highest possible stratigraphic precision for the investigated section, age control was based on two independent lines of evidence: (1) biostratigraphic events and (2) $\delta^{13}C$ stable isotope stratigraphy. The combination of both methods allowed the detection of chronostratigraphic events occurring in connection with the Cenomanian/Turonian boundary and OAE-2. A rough estimate using ages published in Mitchell et al. (2004), Ogg et al. (2004) and Jarvis et al. (2006) resulted in the calculation of sedimentation rates around 0.2 to 0.4 mm/ky with slightly lower values during the black shale interval.

### 4.1. Biostratigraphy

Based on established zonal schemes (e.g., Bralower et al., 1995; Robaszynski and Caron, 1995; Premoli Silva and Verga, 2004) three planktic foraminiferal zones were recognized: *Rotalipora cushmani*-Zone, *Whiteinella archaeocretacea*-Zone, and *Helvetoglobotruncana helvetica*-Zone (Fig. 2). We carefully looked for the first occurrence (FO) of *H. helvetica* in washed residues and thin sections. The occurrence of microfossils in thin sections of the limestone beds is shown in Figure 3. However, the rare occurrence of *H. helvetica* may be easily missed in thin sections and slight differences in its FO in disaggregated samples and in thin sections are possibly caused by the small size and number of the thin sections (only one per sample) examined. The first proven occurrence of the rare *H. helvetica* is from disaggregated samples at about the same level as the FO of the calcareous nannofossil *Quadrum gartneri.* Calcareous nannofossil zonations of Perch-Nielsen (1985) and Burnett (1998) show two or three zones respectively (CC10 to CC11, UC 4 to UC 7, Fig. 2, see Wagreich et al. (2008) for detailed description). Organic-walled microfossils were found in some pilot samples and confirm the age classifications presented here (Pavlishina and Wagreich, 2009).

The calcareous marl below the clay layer that yielded only reworked microfossils (sample RKG-14) contains *R. cushmani, T. greenhornensis* and *T. multiloculata* (in thin sections, Fig. 3) and indicates that the very latest Cenomanian interval (when *T. greenhornensis* already became extinct) is not represented in the Rehkogelgraben. This suggests a stratigraphic gap of, however, only short duration (see also discussion in Wagreich et al. (2008)).

### 4.2 Stable isotope stratigraphy ($\delta^{13}C$)

In addition to the $\delta^{13}C$-measurements on calcareous matter already published in Wagreich et al. (2008) we also obtained $\delta^{13}C$-data of organic matter. The new $\delta^{13}C_{org}$-curve (Fig. 2) shows an increase of more than 2 ‰ between the upper Cenomanian average level and the black shale interval (around –26‰ to almost –23‰). Upsection, the values drop steeply to –28‰ during the basal and lower Turonian. Inclusion of the $\delta^{13}C_{org}$ data enabled us to complete the $\delta^{13}C$-record also for the black shale interval where the $CaCO_3$-content is too low for any $\delta^{13}C_{carb}$-measurements (Fig. 2). Based on this improved data set we were able to correlate the $\delta^{13}C$-curves from the Rehkogelgraben with $\delta^{13}C$-curves from key sections (Eastbourn (England), Gubbio (Italy), Pueblo (USA, also GSSP for the Cenomanian/Turonian boundary)) published in e.g., Tsikos et al. (2004). We used the major positive excursions (peaks P1 to P4) to compile the correlation (Fig. 4). The most prominent peak (P1) is within the thick basal black shale. As at Eastbourne, the $\delta^{13}C_{org}$ excursion of P2 appears earlier than the $\delta^{13}C_{carb}$ peak.

## 5. Results

Comparison of planktic foraminifera and radiolaria abundances indicates the simultaneous decrease of both groups during the late Cenomanian to about 25% of the earlier numbers (Fig. 5). Planktic foraminifera are about 100 times more frequent than radiolaria. The number of radiolaria, however, increases in the latest phase of this interval while planktic foraminifera remain low. Radiolaria are more frequent than planktic foraminifera during the black shale phase of deposition, although both groups occur with low numbers (Fig. 5). Both groups increase in the early Turonian but planktic foraminifera are about 50 times more frequent than radiolaria. However, late Cenomanian abundance levels are not reached within the early Turonian section investigated here. These results correspond largely to those based on thin

sections studied by Wagreich et al. (2008). We assume that these dramatic developments have their causes in fundamental changes in the paleoceanography at that time. We therefore investigated the most prominent microfossil groups in detail, in particular planktic and benthic foraminifera.

The influence of diagenesis on assemblage compositions was apparently low. Even the strata with the highest potential for dissolution (black shales and adjacent layers) show presence of planktic foraminifera (complete calcareous shells), rather high diversities and high proportions of calcareous benthic foraminifera. Severe dissolution would have led to disappearance of species with calcareous shells and strong dominance of arenaceous benthic foraminifera within the assemblages. The thickest (basal) black shale yielded only very few corroded calcareous specimens and we can not completely exclude reworking from older sediments or partial dissolution of specimens with more delicate tests. However, dissolution of calcareous components has completely altered assemblages in other OAE-2 black shales (e.g., at Gubbio, Italy). Furthermore, arenaceous species are relatively rare and of small size at Rehkogelgraben (contrary to deposits of the Rhenodanubian Flysch basin). This points to local environmental conditions as the crucial factor for assemblage compsition and chemical dissolution appears to be negligible. Specimens from the second black shale are just as well preserved as those from pre- or post OAE samples.

### 5.1 Planktic foraminifera

We distinguished between equilibrium species (*K*-strategists), intermediate species and opportunists (*r*-strategists), following the concepts explained in Premoli Silva and Sliter (1999) and Coccioni and Luciani (2004), in order to interpret habitats and changes in nutrient supply. Representative specimens of all recognised planktic foraminiferal species are shown in Figure 6.

The relatively poor state of preservation of microfossils in the washed residues made it necessary to combine a group of *Whiteinella*-species with very similar morphology for counting purposes. *Whiteinella archaeocretacea, W.aprica, W. aumalensis,* and *W. inornata* were lumped together under the name *W. archaeocretacea*, which is probably the most common among these species. Because of their very similar morphology and identical general habit we assume similar ecologic requirements or preferences for these species.

### 5.1.1 Equilibrium species (*K*-strategists)

*Rotalipora* and *Thalmanninella* (Fig. 7A) include *R. cushmani*, *T. deekei* and *T. greenhornensis*. The late Cenomanian samples contain various amounts of these species between 92 to 327 ind/g (or 0.4 to 2.5%). Occasional occurrences of rare "rotaliporids" in one black shale layer and some lower Turonian marl layers (i.e., above $\delta^{13}$Corg-peak 1) are interpreted as reworked from older strata.

*Praeglobotruncana* spp. (Fig. 7B) includes *P. gibba* and *P. stephani*. Numbers vary between 181 and 880 ind/g during the late Cenomanian but their percentages increase slowly from 1 to about 5%. During the black shale interval their number varies between 0 and 1.5 ind/g, i.e., much lower. However, this may corresponds to up to 27% of the assemblage. *Praeglobotruncana* becomes a major component in lower Turonian strata with up to 4300 ind/g (max. 56%).

*Dicarinella* spp. (Fig. 7C) includes *D. canaliculata, D. hagni* and *D. imbricata*. Both, absolute numbers and percentages of this group remain low throughout the investigated section. Maximum values are 62 or 120 ind/g in upper Cenomanian and lower Turonian strata respectively and even below 0.03 ind/g during the black shale interval. Proportions are always below 1%.

### 5.1.2 Intermediate species

*Whiteinella* spp. (Fig. 7D) includes *W. archaeocretacea, W.aprica, W. aumalensis, W.baltica, W. brittonensis* and *W. inornata*. The *Whiteinella* spp. content decreases from more than 9000 to around 2000 ind/g during the late Cenomanian. There is however no distinct decrease in *Whiteinella* if expressed as percentages (6-20%). Directly above the lower thick black shale layer, *Whiteinella* rises abruptly from zero to 32%, but their numbers remain low (max. 3.4 ind/g). Its percentages remain constant during the early Turonian but the absolute numbers increase continuously to pre-black shale levels.

*Hedbergella* spp. (Fig. 8A) includes *H. delrioensis, H. planispira* and *H. simplex*. *Hedbergella* is the major component of late Cenomanian assemblages (9000 to 37000 ind/g or

63 to 80 %). Their numbers decrease drastically during the black shale interval (0.2 to 6.6 ind/g) but percentages remain high (42 to 73 %). One sample of the thick basal black shale layer contains only a single specimen and no other genera. Absolute numbers as well as percentages are much lower during the early Turonian if compared with the late Cenomanian (452 to 2843 ind/g or 22 to 23 %).

### 5.1.3 Opportunists (*r*-strategists)

*Schackoina cenomana* (Fig. 8B) varies with low numbers (0 to 282 ind/g) throughout the section. Its highest percentage (5.3%) is within the black shale interval although the absolute number is very low (0.56 ind/g) and its absolute content is higher below and above.

*Heterohelix* spp. (Fig. 8C) includes *H. moremani* and *H. reussi*. Absolute numbers as well as percentages decrease from 6390 to 425 ind/g (or 11.9 to 2.4%) during the lower portion of the late Cenomanian but slightly increase towards the end of this interval (2143 ind/g or 9.7 %). Their absolute content is low during the black shale interval (0 to 0.5 ind/g or 0 to 5.1 %) and increases slowly to pre-black shale levels during the basal to early Turonian (99 to 1856 ind/g or 2.4 to 15.0 %).

*Gümbelitria cenomana* (Fig. 8D) occurs with low numbers within the section (0 to 416 ind/g or 0 to 2.3 %). However, this species shows a distinct increase towards the end of the late Cenomanian interval but never reaches more than 1381 ind/g or 6.3 %.

## 5.2 Benthic foraminifera

Diversity of assemblages below and above the black shale interval is high (compare Table 2) but decreases within the black shale interval. Parallel to this, the absolute number (ind/g) of benthic foraminifera is markedly reduced. However, black shale interval assemblages do not show a significantly higher proportion of arenaceous species (Fig. 9, left column), which would point to dissolution on the ocean floor during time of deposition. Thus, dissolution hardly plays a role for the species composition of the samples investigated. All important occurring benthic foraminifera are shown in Figure 10.

### 5.2.1 Arenaceous against calcareous species and benthic morphogroups

Percentages of arenaceous foraminifera (Fig. 9) vary around 12% for the late Cenomanian, fluctuate strongly during the black shale interval (0 to 72%) and increase to around 30% during the early Turonian.

The benthic foraminiferal morphogroups listed here are named mostly after genera and their distribution is shown in Figure 9. *Ammobaculites* (including *Bulbobaculites*) has its maximum close to the base of the investigated section (435 ind/g). A further, second peak occurs during the early Turonian (120 ind/g). *Bathysiphon* is only frequent during the late Cenomanian (max. 191 ind/g). *Haplophragmoides* shows two maxima: 258 ind/g at the beginning of the late Cenomanian interval and a smaller maximum in the early Turonian with 60 ind/g. *Reophax* shows higher frequencies in the early Turonian (max. 301 ind/g) than in the late Cenomanian (max. 263 ind/g). *Spiroplectammina* is restricted to the upper part of upper Cenomanian strata (max. 256 ind/g). *Tritaxia* is less frequent (max. 23 ind/g) and restricted to the lower portion of the late Cenomanian part. *Trochammina* is most frequent in the early Turonian part (max. 105 ind/g). Other arenaceous taxa are more or less evenly distributed in the entire section (max. 65 ind/g).

The largest portion among calcareous benthic foraminifera is made up by turrilinids (*Neobulimina, Praebulimina*). Their abundance pattern shows two prominent peaks at the beginning and the end of the late Cenomanian interval (>1800 ind/g) and in the youngest early Turonian sample (584 ind/g). Gavelinellids and *Planulina* combined are generally less frequent but show the greatest abundance of all benthic groups (4104 ind/g) at the base of the Rehkogelgraben section. Elongated nodosariids (*Dentalina, Nodosaria*) are relatively rare throughout the section with a maximum of 76 ind/g during the late Cenomanian. *Gyroidinoides* occurs in almost all samples and reaches maximum abundance (643 ind/g) in the upper portion of the late Cenomanian interval. Lensiform nodosariids (*Lenticulina, Planularia*) are generally rare (max. 18 ind/g). *Gabonita* is only frequent at the base of the section (max. 869 ind/g). *Bolivina* is rather rare (max. 57 ind/g) and is missing in early Turonian samples. Other calcareous species occur with less than 413 ind/g.

### 5.2.2 Trends in size distribution of benthic foraminifera

The investigated section shows a clear tripartite subdivision for the three size fractions analysed (Fig.11). Late Cenomanian and early Turonian samples show high and relatively similar benthic foraminferal numbers in all size fractions. During the black shale interval benthic foraminifera are less abundant. Specimens of the smallest fraction are present in all samples. This is also valid for specimens of the middle fraction but with significantly lower numbers. Specimens of the largest fraction are missing in all but one sample of the black shale interval but occur in almost all samples before and after this interval.

### 5.3 Occurrence of radiolaria

Nasselarian species are extremely rare and only single specimens were found in some samples. The overwhelming majority of specimens belong to the order Spumellaria. Radiolarian distribution in the samples is listed in Table 3. Abundances of radiolaria vary between 53 and 423 ind/g during the late Cenomanian interval. It is from 0.2 to 132 ind/g during the black shale interval and increases again to 91 to 165 ind/g during the early Turonian. Figure 5 clearly shows the inversion of the relation to planktic (and also benthic) foraminifera. The abundances of radiolaria are about two orders of magnitude lower than those for planktic foraminifera during “normal” periods. It is the opposite for the black shale interval. The abundances of radiolaria during the black shale interval (12.7 to 131.6 ind/g) are however still a quarter of those of the late Cenomanian (53 to 423 ind/g). The highly similar curves show unidirectional, coeval fluctuations and approximately constant differences in abundances for radiolaria, benthic and planktic foraminifera on a logrithmic scale.

## 6. Paleoceanographic interpretation and discussion

### 6.1 Environmental changes at the seafloor

Paleo-water depth can be estimated by using ratios of planktic to benthic foraminifera (or percent planktic foraminifera). Proportions of planktic foraminifera outside the black shale interval vary around 90 % and point to bathyal depositional environments (c. 800 to 1000 m paleo-water depth) if compared with modern settings (e.g., van der Zwaan et al., 1990) or estimates for the Cenomanian-Turonian of the Western Interior Basin (Leckie et al., 1998). This confirms the categorization (distal slope) of Wagreich et al. (2008).

The size distribution of benthic foraminifera points to a clear tripartite subdivision of the section investigated which can be used to interpret bottom-water oxygenation (Fig. 11). High numbers of small, medium and large specimens indicate oxic conditions for the late Cenomanian interval. The black shale interval is characterized by very low numbers of small specimens and absence of larger forms, pointing to low oxic or even dysoxic conditions during OAE-2. Oxic conditions re-appear during the early Turonian, indicated by high numbers of small and large benthic foraminifera.

Species belonging to the tapered (turrilinids, *Gabonita*), elongated flattened (*Bolivina*) and flatteded trochospiral (small gavelinellids) morphogroups are frequent in the late Cenomanian portion of the Rehkogelgraben section. In combination with the high number of "large" benthic specimens, we interpret this as a food-rich but moderately oxygenated setting. High abundances of planktic foraminifera confirm this conclusion. Nutrient supply was probably lower in the early Turonian, indicated by lower total numbers and very restricted occurrences of *Gabonita* and *Bolivina*. The black shale interval shows the lowest abundances, going down to 1/1000 or less of late Cenomanian rates (Table 4, Fig. 5). The assemblages of small sized specimens are relatively diverse and contain A*mmobaculites, Haplophragmoides, Bolivina, Reophax*, gavelinellids, *Gyroidinoides* and some *Bathysiphon* and turrilinids. *Gabonita* does not occur in these samples. Although the total organic carbon content is relatively high in the black shales, the extremely low abundances and the absence of *Gabonita* and rareness of other high productivity indicators (e.g., *Bolivina*, turrilinids) point to very low surface productivity and subsequent food supply to the seafloor combined with low oxic to dysoxic conditions.

### 6.2 Environmental changes in surface waters

Similar to bottom-water conditions, a tripartite subdivision is reported for surface waters. Moderate numbers of mesotrophic (*Praeglobotruncana*) to highly oligotrophic (*Rotalipora, Thalmanninella*) equilibrium species are characteristic for the late Cenomanian portion of the Rehkogelgraben section. Presence of the deep dwellers also indicates the absence, or a very deep upper surface of an oxygen minimum zone (i.e., far below thermocline). Also the low numbers of stress tolerant *Heterohelix* and *Gümbelitria* point to stable conditions with limited nutrient supply. The latter genus becames a little more frequent (<7%) in the last samples of this interval, but never reached levels indicative of eutrophication and highly oligotrophic

species are still present. The assemblages are complemented by hedbergellids and whiteinellids. The high productivity indicator *Schackoina* is always very rare. Thus, an oligotrophic regime is assumed for the late Cenomanian at Rehkogelgraben.

The black shale interval (representing OAE-2) is characterized by very low numbers of planktic foraminifera. Spumellarian radiolaria are more frequent than planktic foraminifera but also significantly less frequent than in previous and successive periods. Figure 12 shows reduced diversity and number of specimens in the thick lower black shale layer, but a higher number of species and a lower amount of individuals in the marly clay layer above. This pattern is repeated in the next black shale/marly clay couplet. Here, the percentage of (and also numbers of) *Schackoina* is the highest (5.3%). This pattern points to higher nutrient availability during times of black shale deposition than during marly clay-periods, although there were apparently neither distinct eutrophication events leading to blooms of indicator species such as *Schackoina* nor increased numbers of stress indicating *Heterohelix* or *Gümbelitria*. The low numbers of *Heterohelix* and absence of a "*Heterohelix* shift" to dominance with the onset of OAE-2 (e.g., Leckie et al, 1998; Keller et al., 2008) suggest that the upper water column was not nearly as stressed as observed at other localities (see chapter 6.4). The slightly increased number and percentage of *Schackoina* in one sample does not point to eutrophic or mesotrophic conditions (compare data published by e.g., Coccioni and Luciani (2004)). The thin marly clay-layer directly above the third black shale layer yielded an already rather diverse (six genera), but individual poor assemblage with an almost “normal” species composition. This assemblage may already indicate the re-establishment of stable oligotrophic conditions. Also the fact that radiolaria are now again less common than benthic and planktic foraminifera (Fig. 5) point to a return to almost pre-OAE conditions.

Early Turonian post-OAE assemblages became more and more specimen-rich and reached pre-OAE levels during the *H. helvetica*-Zone. Already during the recovery phase, the assemblages are dominated by mesotrophic *Praeglobotruncana* and *Whiteinella*. Although rare, *Dicarinella* became more frequent than during the late Cenomanian. Thus, stable, well-oxygenated conditions must have prevailed down to thermocline depths. *Heterohelix* varies around 10 %, and *Gümbelitria* and *Schackoina* occur with very low numbers. Therefore, surface productivities similar to pre-OAE-levels were not re-established before the beginning of the *H. helvetica*-Zone. Based on ages published in Ogg et al. (2004), a period of about 300 ky was needed to re-establish a planktic carbonate-producing regime.

### 6.3 Foraminifera, radiolaria and paleo-productivity

The curve progressions of benthic and planktic foraminifera and of radiolaria (Fig. 5) point to a strong coupling of the frequencies of these groups during the periods before and after the black shale interval. Radiolaria and planktic foraminifera depend on prey such as diatoms, coccolithophores or other algae and bacteria (e.g., Brasier, 1980; Hemleben et al., 1989; Murray, 1991; Leckie et al., 2002), and deep-sea benthic foraminifera on the organic rain that reaches the seafloor (e.g., van der Zwaan et al., 1999; Gooday, 2003). Thus, abundances of radiolaria, planktic and benthic foraminifera can be used to estimate changes in surface (paleo-) productivity. We assume sufficiently stable paleoceanographic conditions that facilitated the sedimentation of calcareous deposits (i.e., limestones and marls) during pre- and post-black shale periods. The cause for the coupling may be found in general primary productivity changes in the region.

At Rehkogelgraben, the ecologic crisis during OAE-2 is expressed by extremely low and erratically fluctuating abundances of planktic and benthic foraminifera and, most prominent, c. 10 times higher abundance values for radiolaria than for foraminifera (Fig. 5). Compared with the late Cenomanian interval, the pelagic eco-system was able to sustain significantly lower numbers of radiolaria and foraminifera during the early Turonian, probably an aftermath of OAE-2.

### 6.4 Comparison with other deep-water sites

The impact of OAE's is assumed to be widespread, if not global (e.g., Schlanger et al., 1987). Similar faunal consequences are asumed for similar paleoceanographic and paleoecologic conditions. Therefore, we compared the micro-faunal successions of selected key sections in order to classify the Rehkogelgraben record or to show its peculiarity.

The Bonarelli Level represents the OAE-2 in northern Italy (Gubbio; Fig. 1). Many differences exist with the Rehkogelgraben section. The black shales are mainly devoid of carbonates and very rare planktic foraminifera occur as silicified ghosts (Premoli Silva et al., 1999). Nannofossil assemblages and a relative increase in *Schackoina* (up to > 50%, Coccioni and Luciani (2004)) indicate increased surface fertility shortly before the event. The higher

surface productivity is possibly related to upwelling. A slow recovery of planktic foraminiferal assemblages, represented by scattered *Heterohelix* and *Hedbergella*, follows the black shale. Percentages of praeglobotruncanids and whiteinellids are constantly low. The Bonarelli Level itself is devoid of benthic foraminifera, but so-called Deep-Water Agglutinated Foraminifera (DWAF) are common below and above the Bonarelli level (Coccioni et al., (1995) in Premoli Silva et al., (1999)). Furthermore, radiolaria of the black shales are dominated by deep-dwelling Nasselaria. Similar to Rehkogelgraben are a general dominance of *Hedbergella*, low frequencies of *Heterohelix* before and after the event, and relatively low percentages of rotaliporids in the pre-OAE-2 interval. Coccioni and Luciani (2004) propose an extremely stressed environment with a very much expanded oxygen minimum zone and a highly eutrophic surface layer for the Bonarelli Level. Increased surface productivity (*Schackoina*-bloom) and an enhanced oxygen minimum zone characterize the pre-OAE phase, while environmental perturbations continued long after the event, very different from what is shown for the Rehkogelgraben section.

The record of Roter Sattel in Switzerland (Romandes Prealps, Strasser et al. (2001)) near the southwestern end of the Penninic Ocean is similar to Gubbio in many ways (absence of planktic foraminifera in black shale interval, dominance of radiolaria) but differs from the Rehkogelgraben record by its high terrigenous influx (quartz, higher plant organic matter). Sediments of Roter Sattel were deposited on a platform (terrain, Briançonnais Domain).

Identification of OAE's by microfaunas is difficult at permanent upwelling sites with constantly high surface productivity like, e.g., the northwestern African magin. Foraminiferal assemblages from the Tarfaya Basin are characterized by successively lower diversities and restriction to dysoxic indictors (dominantly *Neobulimina albertensis* and occasional *Praebulimina*, *Gabonita* and small *Gavelinella* specimens) as a consequence of successive subsidence and cyclic eustatic onlap of oxygen-depleted bottom waters (Gebhardt et al., 2004). The onset of OAE-2, as indicated by the $\delta^{13}C$ excursion (Kuhnt et al., 2005), could not be traced by changes in benthic foraminiferal assemblages. In contrast, the planktic assemblages at Tarfaya show a severe impact on the diversity, as well as the permanent dominance of *Hedbergella planispira* and *Heterohelix moremani* across the boundary interval, a *Heterohelix*-shift shortly after the extinction of rotaliporids and persistent also into the early Turonian *H. helvetica*-Zone, and a short *Gümbelitria*-bloom preceeding the

*Heterohelix*-shift (Keller et al., 2008). All these differences point to a completely dissimilar initial situation when compared to the Rehkogelgraben section.

Sediments from the Demerara Rise (Central Atlantic Ocean) consist entirely of black shales with up to 29% TOC during OAE-2 (Erbacher et al., 2005) and were deposited in 500 to 1000 m water depth (Friedrich et al., 2008b). The benthic foraminiferal assemblages show low diversities and are dominated by high productivity - dysoxic/anoxic indicators (*Bolivina*, *Gavelinella*, buliminids). The deepest of several sites indicates the most oxygenated bottom waters before OAE-2, while anoxic to dysoxic conditions prevailed in shallower sites, pointing to a position within an oxygen minimum zone (Friedrich et al., 2006). A strengthened oxygen minimum zone further reduced oxygenation, i.e., almost complete disappearance of benthic foraminifera in the shallow sites, but did not led to complete anoxia in the deepest site during the OAE. Pre-OAE conditions returned after the carbon isotope excursion with a further weakening of the oxygen minimum zone later on. The abundances of benthic foraminifera (ind/g) were in the same range as at Rehkogelgraben, but the assemblages were much less diverse and restricted to eutrophication indicators (Friedrich et al., 2006). Cenomanian to Coniacian geochemical proxies and Turonian planktic foraminiferal assemblages from Demerara Rise consisting of abundant hedbergellids and heterohelicids with rare specimens of *Pseudoguembelina*, *Marginotruncana* and *Clavihedbergella* (Friedrich et al., 2008a) and point to extremely high sea-surface temperatures (Norris et al., 2002; Wilson et al., 2002; Bice et al., 2006; Bornemann et al., 2008). Assemblages dominated by clavate planktic foraminifera and *Heterohelix pulchra* are interpreted to represent the phases with the highest surface productivity (Friedrich et al., 2008a). Similar assemblages do not occur at Rehkogelgraben. The records from Tarfaya and Demerara Rise represent a paleoceanographic setting with extremly high surface productivity during OAE-2 and even before and after the event. This setting can therefore not serve as a model for the interpretation of the Rehkogelgraben record.

The incomplete section at Blake Nose (0.5 My of OAE-2 are missing, including organic rich sediments, Huber et al. (1999)) shows dominance of hedbergellids (in combination with *Whiteinella*) in the pre-OAE interval and a change to biserial forms after OAE-2 (*Heterohelix*-shift). As at Rehkogelgraben, keeled morphotypes are more frequent in post-OAE sediments. Rotaliporids are also relatively rare but dicarinellids are much more frequent throughout. In contrast to Rehkogelgraben, helvetoglobotruncanids contribute significantly to

643 the planktic assemblages in the early Turonian interval. Also as at Rehkogelgraben, no
644 significant amounts of *Schackoina* were recorded. The similarities between Blake Nose and
645 Rehkogelgraben may be explained by almost equal paleo-latitudes (Fig. 1), the differences by
646 the less restricted location of Blake Nose in the far larger North Atlantic Ocean. Assemblages
647 and abundance pattern similar to Rehkogelgraben (but without a distinct black shale interval)
648 were also recorded from Tibet, i.e., the southern margin of the Tethyan Ocean at that time
649 (Wan et al., 2003), pointing to similar ecological conditions at least for pre- and post-OAE
650 sediments.
651
652 **6.5 A special paleoceanographic situation in the Penninic Ocean**
653
654 Erbacher et al. (1996) described a general model for the formation of OAEs during the mid-
655 Cretaceous. The productivity-driven OAE-2 at the Cenomanian/Turonian boundary was
656 probably caused (among other factors) by a high sea level leading to leaching of nutrients
657 from coastal lowlands and subsequent increased productivity (see Mort et al. (2007) for role
658 of phosphorus). This in turn caused the expansion of the oxygen minimum zone (e.g., Leckie
659 et al., 2002) with coeval reduction of ecological niches and extinction events for both planktic
660 and benthic dwellers, e.g., rotaliporids among planktic foraminifera. Dominance of type 2
661 kerogen is thought to be indicative for increased (marine surface) productivity (Jenkyns et al.,
662 1994). This indicator is present in the black shale interval at Rehkogelgraben (Wagreich et al.,
663 2008). However, the planktic and benthic foraminiferal assemblages found at Rehkogelgraben
664 do not confirm such a depositional system. Thus, a different concept is required for the
665 Penninic Ocean.
666
667 Modern paleogeographic reconstructions for around 94 Ma (e.g, Kuypers et al., 2002;
668 Friedrich et al., 2006; Mort et al., 2007, 2008; www.scotese.com/cretaceo) show the Penninic
669 Ocean as an almost completely enclosed deep basin (Fig. 1). This special bathymetric
670 situation may play a key role for the explanation of the apparent differences between the high
671 productivity in most parts of the world ocean and the overall absence of high productivity
672 indicators in the foraminiferal assemblages at Rehkogelgraben during OAE-2. The increased
673 nutrient flux and related increased productivity recorded in the adjacent oceans (Kuypers et
674 al., 2002; Mort et al., 2007) has probably not reached the northern part of the Penninic Ocean,
675 but an oxygen minimum zone developed in this region. This explains coeval low
676 foraminiferal abundances and absence of increased numbers of high productivity indicators

677 such as *Gabonita* (benthic) or *Heterohelix* and *Schackoina* (planktic) during the black shale
678 interval. Dysoxic bottom-water conditions are assumed for adjacent seas (Mort et al., 2007) as
679 well as for the Penninic Ocean (this study). First results of palynological investigations on
680 samples from the Rehkogelgraben also point to anoxic/dysoxic conditions rather than to high
681 productivity (Pavlishina and Wagreich, 2009). Causes for the recorded pattern may include:
682 1) a generally west-east oriented coast line in the north and low air pressure systems that did
683 not allow for upwelling equivalent to modern and ancient settings along the western coasts of
684 continents (Parrish and Curtis, 1982). Atmospheric General Circulation Models (GCM)
685 predict low wind stress and current velocities as well as predominance of a low air pressure
686 system in the region of the Penninic Ocean for the Turonian, both unfavorable for the
687 development of upwelling cells (Poulsen et al., 1999, 2001; Flögel, 2002). 2) Absence of
688 large continents in the surrounding of the Penninic Ocean that could supply the sea with
689 nutrients from river runoff (Fig. 1). 3) Surface current driven removal of leached nutrients
690 from the flooded shelves away from the Penninic Ocean.
691
692 We speculate that the already restricted water exchange with the Tethys was further reduced
693 during the OAE. A somewhat more sluggish circulation related to higher temperatures in
694 greater water depths and weakened temperature gradients (e.g., Huber et al., 1999; Friedrich
695 et al., 2008b) in adjacent Tethys and North Atlantic Ocean might have been a sufficient cause
696 and stored nutrients were used up in the Penninic Ocean, resulting in the recorded low-
697 productivity microfossil assemblages. The OAE had a less severe impact on the diversity of
698 planktic and benthic foraminifera than in upwelling areas as, e.g., the deeper part of the
699 Tarfaya Basin (no benthic and only two planktic species were recorded by Keller et al.
700 (2008)) or the Demerara Rise (Friedrich et al., 2006). We recorded 1-3 planktic and 1-5
701 benthic taxa per sample in the thick black shale layer at the base of the OAE and even 8-15
702 planktic and 12-15 benthic taxa per sample above but still within the black shale interval at
703 Rehkogelgraben. The Penninic Ocean may have even served as a refuge for some of these
704 species during the environmental crisis elsewhere.
705
706 Increased $CO_2$-uptake of the ocean, derived from large igneous province activity, played an
707 important role in the formation of OAE-2 (Kerr, 1998; Huber et al., 1999), or at least
708 preconditioned the climatic and oceanic regimes (Ando et al., 2009). This might account for
709 part of the dysoxic bottom-water conditions reported at Rehkogelgraben and elsewhere.
710 Increased $pCO_2$ may have also led to acidification of large portions of the water column and

subsequent difficulties in carbonate secretion for foraminifera (Moy et al. (2009), with other references therein). Radiolaria with their silica skeletons were possibly less affected by acidification and had a competitive advantage against organisms secreting a carbonate shell, leading to the reversals in the recorded radiolaria to foraminifera ratios.

## 7. Conclusions

The Rehkogelgraben section shows a tripartite subdivision for surface and bottom waters. High numbers of mesotrophic to highly oligotrophic planktic foraminiferal species and low numbers of stress tolerant species are characteristic for the late Cenomanian and indicate an oligotrophic regime in the upper water column. The black shale interval representing OAE-2 is characterized by very low numbers and relatively high diversities of planktic foraminifera. High productivity indicators do not form significant propotions within the assemblages. Post-OAE assemblages are dominated by mesotrophic species and reduced surface productivities similar to pre-OAE-levels were re-established. About 300 ky were needed to re-establish an effective pelagic carbonate-producing regime.

High numbers of small to large benthic foraminifera and frequent high nutrient-flux indicators point to oxic and food-rich conditions on the late Cenomanian seafloor. The black shale interval showed the lowest abundances, going down to 1/1000 or less of late Cenomanian values. The assemblages are characterized by low numbers of small specimens and absence of larger forms, pointing to low oxic or dysoxic conditions. Oxic conditions re-appeared during the early Turonian, indicated by high numbers of small and large benthic foraminifera. Nutrient supply was probably lower in the early Turonian if compared with the late Cenomanian, indicated by lower total numbers and very restricted occurrences of high nutrient-flux indicators.

Abundances of planktic foraminifera were about one order of magnitude higher than those of benthic foraminifera, and those in turn one order of magnitude higher than those of radiolaria. The regular coupling of abundances indicates strong dependences within the ecologic system during the stable late Cenomanian and early Turonian periods. This system was less efficient during the early Turonian if compared with the late Cenomanian period, probably an aftermath of the ecologic crisis at the Cenomanian/Turonian boundary. The ecologic crisis during OAE-2 is expressed by extremely low and erratically fluctuating abundances of

745 planktic and benthic foraminifera and c. 10 times higher abundances for radiolaria than for
746 foraminifera.
747
748 Overall, the Rehkogelgraben record points to unusual paleoceanographic conditions during
749 the OAE-2. We assume that the paleogeographic and bathymetric situation of the Penninic
750 Ocean (semi-enclosed basin) played a key role for the explanation of the apparent differences
751 between the high surface productivity in most parts of the world ocean and the overall
752 absence of high productivity indicators in the foraminiferal assemblages at Rehkogelgraben.
753 The record reported here suggests that high surface productivity during OAE-2 was not a
754 global phenomenon in oceanic settings and it might be worth to look for other sites with
755 similar conditions.
756
757 If compared with Cenomanian-Turonian boundary sections with black shale intervals
758 elsewhere, the Rekogelgraben record shows much higher benthic and planktic foraminiferal
759 diversities during OAE-2. The Penninic Ocean may therefore have even served as a refuge
760 during the environmental crisis.
761
762 **Acknowledgements**
763
764 Markus Kogler (GBA) is thanked for picking and counting radiolarians. We thank Mike
765 Bolshow and Shir Akbari (both NOCS) for $\delta^{13}C_{org}$ sample preparation and analyses. Mark
766 Leckie and an anonymus reviewer made valuable suggestions to improve the manuscript.
767 Micheal Wagreich acknowledges financial support by FWF Joint Seminar AJS 308-B17 and
768 IGCP 555 "Rapid Environmental/Climate Change in the Cretaceous Greenhouse World:
769 Ocean-Land Interactions". Lindsey Fox acknowledges receipt of an Undergraduate Research
770 Bursary (2009) from The Nuffield Foundation. This study was partly funded by the
771 European Commission while Oliver Friedrich held a Marie Curie Intra-European Fellowship
772 at the University of Southampton (project PLIO-CLIMATE) and finished while he held an
773 Emmy-Noether Research grant of the DFG (FR 2544/2-1).
774
775 **Appendix :** List of identified taxa. Reworked specimens from sample REH 4/1 are not
776 included.
777
778 1. Planktic foraminifera

*Clavihedbergella moremani* (Cushman 1931)
*Dicarinella canaliculata* (Reuss 1854)
*Dicarinella hagni* (Scheibnerova 1962)
*Dicarinella imbricata* (Mornod 1949)
*Eohastigerinella subdigitata* (Carman 1927)
*Gümbelitria cenomana* (Keller 1935)
*Hedbergella delrioensis* (Carsey 1926)
*Hedbergella planispira* (Tappan 1940)
*Hedbergella simplex* (Morrow 1934)
*Helvetoglobotruncana helvetica* (Bolli 1945)
*Helvetoglobotruncana praehelvetica* (Trujillo 1960)
*Heterohelix moremani* (Cushman 1938)
*Heterohelix globulosa* (Ehrenberg 1840)
*Heterohelix reussi* (Cushman 1938)
*Marginotruncana marginata* (Reuss 1845)
*Marginulina* sp. cf. *M. renzi* (Gandolfi 1942)
*Praeglobotruncana gibba* Klaus 1960
*Praeglobotruncana stephani* (Gandolfi 1942)
*Rotalipora cushmani* (Morrow 1934)
*Schackoina cenomana* (Schacko 1897)
*Thalmanninella deekei* (Franke 1925)
*Thalmanninella greenhornensis* (Morrow 1934)
*Thalmanninella multiloculata* (Morrow 1934)
*Whiteinella aprica* (Loeblich and Tappan)
*Whiteinella archaeocretacea* Pessagno 1967
*Whiteinella baltica* Douglas and Rankin 1969
*Whiteinella brittonensis* (Loeblich and Tappan 1961)

2. Benthic foraminifera
*Ammobaculites* sp. cf. *A. amabilis* Fuchs 1967
*Ammobaculites fragmentarius* Cushman 1927
*Ammobaculites subcretacea* Cushman and Alexander 1930
*Ammobaculoides mosbyensis* Eicher 1965
*Ammodiscus cretaceus* Reuss 1845

813 *Ammomarginulina lorangerae* Stelck and Wall 1955
814 *Ammosphaeroidina sphaeroidiniformis* (Brady 1884)
815 *Bathysiphon* spp.
816 *Berthelina dakotensis* Fox 1954
817 *Bolivina anambra* Petters 1982
818 *Bolivina* sp. cf. *B. incrassata* Reuss 1851
819 *Bulbobaculites problematicus* (Neagu 1962)
820 *Cibicides beaumontianus* (d'Orbigny 1840)
821 *Dentalina catenula* Reuss 1860
822 *Dentalina marginuloides* Reuss 1851
823 *Eouvigerina cretae* (Ehrenberg 1854)
824 *Eouvigerina* sp.
825 *Gabonita* cf. *ogugensis* Petters 1982
826 *Gavelinella* spp.
827 *Gyroidinoides lenticulus* (Reuss 1845)
828 *Gyroidinoides umbilicatus* (d'Orbigny 1840)
829 *Haplophragmoides excavatus* Cushman and Waters 1927
830 *Haplophragmoides rugosa* Cushman and Waters 1927
831 *Haplophragmoides* sp. cf. *H. walteri* (Grzybowski 1898)
832 *Haplophragmium* sp.
833 *Hyperammina gaultina* ten Dam 1950
834 *Kalamopsis* sp.
835 *Lenticulina exarata* (v. Hagenow 1842)
836 *Lenticulina gaultina* (Berthelin 1880)
837 *Lenticulina marcki* (Reuss 1860)
838 *Lenticulina pulchella* (Reuss 1863)
839 *Lenticulina saxocretace*a Bartenstein 1955
840 *Marssonella oxycona* (Reuss 1860)
841 ?*Martinottiella* sp.
842 *Neobulimina albertensis* (Stelck and Wall 1954)
843 *Nodosaria* sp.
844 *Nonionella* sp. cf. *N. robusta* Plummer 1931
845 *Osangularia cordieriana* (d'Orbigny 1840)
846 *Osangularia* sp.

*Planularia. complanata* (Reuss 1845)

*Planularia dissona* Plummer 1931

*Planularia* sp. cf. *P. umbonata* Loetterle 1937

*Planulina stelligera* Marie 1941

*Planulina texana* Cushman 1938

*Plectina pinswangensis* Hagn 1953

*Pleurostomella subnodosa* Reuss 1860

*Praebulimina* sp.

*Praebulimina robusta* (de Klasz, Magné and Rérat 1963)

*Praebulimina ventricosa* (Brotzen 1936)

*Psammosphaera fusca* Schulze 1875

*Pullenia minuta* Cushman 1936

*Pullenia reussi* Cushman and Todd 1943

*Ramulina aculeata* (d'Orbigny 1840)

*Recurvoides* spp.

*Reophax minuta* Tappan 1940

*Reophax splendida* Grzybowski 1898

*Rotalia polyrraphes* Reuss 1845

*Saccammina alexanderi* Loeblich and Tappan 1950

*Saccammina globosa* Crespin 1963

*Scheibnerova* sp.

*Spiroplectammina roemeri* Lalicker 1935

*Tappanina laciniosa* Eicher and Worstell 1970

*Tritaxia gaultina* (Morozova 1948)

*Trochammina* sp. cf. *T. depressa* Lozo 1944

*Trochammina umiatensis* Tappan 1957

*Trochamminoides variolarius* (Grzybowski 1898)

*Trochamminoides* sp.

*Verneuilina münsteri* Reuss 1854

**References**

Ando, A., Nakano, T., Kaiho, K., Kobayashi, T. Kokado, E., Khim, B.-H., 2009. Onset of seawater $^{87}Sr/^{86}Sr$ excursion prior to Cenomanian-Turonian Oceanic Anoxic Event 2? New

Late Cretaceous strontium isotope curve from the Central Pacific Ocean. J. Foram. Res. 39, 322-334.

Bernhard, J.M., 1986. Characteristic assemblages and morphologies of benthic foraminifera from anoxic, organic-rich deposits: Jurassic through Holocene. J. Foram. Res. 16, 207-215.

Bice, K.L.,Birgel, D., Meyers, P.A., Dahl, K.A., Hinrichs, K.-U., Norris, R.D., 2006. A multiple proxy and model study of Cretaceous upper ocean temperatures and atmospheric $CO_2$ concentrations. Paleoceanography 21, PA2002, doi: 10.1029/2005PA001203.

Bornemann, A., Norris, R.D., Friedrich, O., Beckmann, B., Schouten, S., Sinninghe Damsté, J.S.,Vogel, J., Hofman, P., Wagner, T., 2008. Isotopic evidence for glaciation during the Cretaceous Supergreenhouse. Science 319, 189-192.

Bralower, T.J., Leckie, R.M., Sliter, W.V., Thierstein, H.R., 1995. An integrated Cretaceous microfossil biostratigraphy. SEPM Spec. Publ. 54, 65-79.

Brasier, M.D., 1980. Microfossils. 193 pp., George Allen and Unwin Ltd, London.

Burnett, J.A., 1998. Upper Cretaceous. In: Bown, P.R. (Ed.), Calcareous nannoplankton biostratigraphy. Chapman and Hall, Kluver Academic Publishing Group, London, pp. 132-199.

Coccioni, R., Luciani, V., 2004. Planktonic foraminifera and environmental changes across the Bonarelli Event (OAE 2, latest Cenomanian) in its type area: a high-resolution study from the Tethyan reference Bottacione Section (Gubbio, central Italy). J. Foram. Res. 34, 109-129.

Coccioni, R., Luciani, V., Marsili, A., 2006. Cretaceous oceanic anoxic events and radially elongated chambered planktonic foraminifera: Paleoecological and paleoceanographic implications. Palaegeogr., Palaeoclimatol., Palaeoecol. 235, 66-92.

Coxall, H.K., Wilson, P.A., Pearson, P.N., Sexton P.F., 2007. Iterative evolution of digitate planktonic foraminifera. Paleobiology 33, 495-516.

915 Elder, W.P., 1989. Molluscan extinction patterns across the Cenomanian - Turonian Stage
916 boundary in the western interior of the United States. Paleobiology 15, 299-320.
917
918 Erbacher, J., Thurow,J., Littke, R., 1996. Evolution patterns of radiolaria and organic matter
919 variations: A new approach to identify sea-level changes in mid-Cretaceous pelagic
920 environments. Geology 24, 499-502.
921
922 Erbacher, J., Friedrich, O., Wilson, P.A., Birch, H., Mutterlose, J., 2005. Stable organic
923 carbon isotope stratigraphy across Oceanic Anoxic Event 2 of Demerara Rise, western
924 tropical Atlantic. Geochem., Geophys., Geosyst. 6, Q0610, doi:10.1029/2004GC000850.
925
926 Fassell, M.L., Bralower, T.J., 1999. Warm, equable mid-Cretaceous: Stable isotope evidence,
927 GSA Spec. Pap. 332, 121-142.
928
929 Fatela, F., Taborda, R., 2002. Confidence limits of species proportions in microfossil
930 assemblages. Mar. Micropaleontol. 45, 169-174.
931
932 Faupl. P., Wagreich, W., 2000. Late Jurassic to Eocene palaeogeography and geodynamic
933 evolution of the Eastern Alps. Mitt. Österr. Geol. Ges. 92, 79-94.
934
935 Flögel, S., 2002. On the influence of precessional Milankovitch cycles on the Late Cretaceous
936 climate systems: comparison of GCM-results, geochemical, and sedimentary proxies for the
937 Western Interior Seaway of North America. Published Ph.D. Thesis, Christian Albrechts
938 Universität zu Kiel, Elektronische Dissertationen, 236 pp., Kiel, Germany.
939
940 Friedrich, O., Erbacher, J., Mutterlose, J., 2006. Paleoenvironmental changes across the
941 Cenomanian/Turonian Boundary Event (Oceanic Anoxic Event 2) as indicated by benthic
942 foraminifera from the Demerara Rise (ODP Leg 207). Rev. Micropaléontol. 49, 121-139.
943
944 Friedrich O., Norris, R.D., Bornemann, A., Beckmann, B., Pälike, H., Worstell, P., Hofmann,
945 P., Wagner, T., 2008a. Cyclic changes in Turonian to Coniacian planktic foraminiferal
946 assemblages from the tropical Atlantic Ocean. Mar. Micropaleontol. 68, 299-313.
947

948 Friedrich O., Erbacher, J., Moriya, K., Wilson, P.A., Kuhnert, H., 2008b. Warm saline
949 intermediate waters in the Cretaceous tropical Atlantic Ocean. Nature Geosci. 1, 453-457.
950
951 Gebhardt, H., 1997. Cenomanian to Turonian foraminifera from Ashaka (NE Nigeria):
952 quantitative analysis and palaeoenvironmental interpretation. Cret. Res. 18, 17-36.
953
954 Gebhardt, H., 1999. Cenomanian to Coniacian biogeography and migration of North and
955 West African ostracods. Cret. Res. 20, 215-229.
956
957 Gebhardt, H., 2006. Resolving the calibration problem in Cretaceous benthic foraminifera
958 paleoecological interpretation: Cenomanian to Coniacian assemblages from the Benue Trough
959 analysed by conventional methods and correspondence analysis. Micropaleontol. 52, 151-176.
960
961 Gebhardt, H., Kuhnt, W., HolbournA., 2004. Foraminiferal response to sealevel change,
962 organic flux and oxygen deficiency in the Cenomanian of the Tarfaya Basin, southern
963 Morocco. Mar. Micropalaeontol. 53, 133-158.
964
965 Gooday, A.J., 2003. Benthic Foraminifera (Protista) as tools in deep-water
966 palaeoceanography: environmental influences on faunal characteristics. Adv. Mar. Biol. 46,
967 1-90.
968
969 Haq, B.U., Hardenbol, J., Vail, P.R., 1987. Chronology of fluctuating sea levels since the
970 Triassic. Science 235, 1156-1166.
971
972 Hart, M.B.,1999. The evolution and biodiversity of Cretaceous planktonic foraminifera.
973 Geobios 32, 247-255.
974
975 Hart, M.B., Bailey, H.W., 1979. The distribution of planktonic Foraminiferida in the mid-
976 Cretaceous of NW Europe. In: Wiedmann, J. (Ed.), Aspekte der Kreide Europas, vol. 6, IUGS
977 Series A, Stuttgart, pp. 527-542.
978
979 Holbourn, A., Kuhnt, W., El Albani, A., Pletsch, T., Luderer, F., Wagner, T., 1999. Upper
980 Cretaceous palaeoenvironments and benthonic foraminiferal assemblages of potential source
981 rocks from the western African margin, Central Atlantic. In: Cameron, N.R., Bate, R.H.,

Clure, V.S. (Eds.), The oil and gas habitats of the South Atlantic. Geol. Soc. London, Spec. Publ., 153, London, pp. 195-222.

Hemleben, C., Spindler, M., Anderson, O.R., 1989. Modern planktonic foraminifera. 363 pp., Springer Verlag, New York.

Houston, R.M., Huber, B.T., Spero, H.J., 1999. Size-related isotopic trends in some Maastrichtian planktic foraminifera: methodological comparisons, intraspecific variability, and evidence for photosymbiosis. Mar. Micropaleontol. 36, 169-188.

Huber, B.T., Hodell, D.A., Hamilton, C.P., 1995. Middle - Late Cretaceous climate of the southern high latitudes: Stable isotopic evidence for minimal equator-to-pole thermal gradients. GSA Bull. 107, 1164-1191.

Huber, B.T., Leckie, R. M., Norris, R.D., Bralower, T.J., CoBabe, E., 1999. Foraminiferal assemblage and stable isotopic change across the Cenomanian-Turonian boundary in the subtropical North Atlantic. J. Foram. Res. 29, 392-417.

Jarvis, I., Carson, G.A., Cooper, M.K.E., Hart, M.B., Leary, P.N., Tocher, B.A., Horne, D., Rosenfeld, A., 1988. Microfossil assemblages and the Cenomanian-Turonian (late Cretaceous) Oceanic Anoxic Event. Cret. Res. 9, 3-103.

Jarvis, I., Gale, A.S., Jenkyns, H.C., Pearce, M.A., 2006. Secular variation in Late Cretaceous carbon isotopes: a new δ13C carbonate reference curve for the Cenomanian-Campanian (99.6-70.6 Ma). Geol. Mag. 143, 561-608.

Jenkyns, H.C., Gale, A.S., Corfield,R.M., 1994. Carbon- and oxygen-isotope stratigraphy of the English Chalk and Italian Scaglia and its paleoclimatic significance. Geol. Mag. 131, 1-34.

Kaiho, K., 1994. Benthic foraminiferal dissolved-oxygen index and dissolved-oxygen levels in the modern ocean. Geology 22, 719-722.

Kaiho, K., 1999. Effect of organic carbon flux and dissolved oxygen on the benthic foraminiferal oxygen index (BFOI). Mar. Micropaleontol. 37, 67-76.

Kaminski, M.A., Kuhnt, W., Moullade, M., 1999. The evolution and paleobiogeography of abyssal agglutinated foraminifera since the Early Cretaceous: A tale of four faunas. N. Jb. Geol. Paläontol., Abh. 212, 401-439.

Keller, G., Pardo, A., 2004. Disaster opportunists Guembelitrinidae: index for environmental catastropes. Mar. Micropaleontol. 53, 83-116.

Keller, G., Adatte, T., Berner, Z., Chellai, E.H., Stueben, D., 2008. Oceanic events and biotic effects of the Cenomanian-Turonian anoxic event, Tarfaya Basin, Morocco. Cret. Res. 29, 976-994.

Kerr, A.C., 1998. Oceanic plateau formation: a cause of mass extinction and black shale deposition around the Cenomanian-Turonian boundary? J. Geol. Soc. London 155, 619-626.

Kollmann, H.A., Summesberger, H., 1982. Excursions to Coniacian - Maastrichtian in the Austrian Alps., Working Group on Cretaceous Stage Boundaries, 4th Meeting, Vienna, 104 pp.

Kolonic, S., Wagner, T., Forster, A., Sinninghe Damsté, J.S., Walsworth-Bell, B., Erba, E., Turgeon, S., Brumsack, H.-J., Chellai, E.H., Tsikos, H., Kuhnt, W., Kuypers, M.M.M., 2005. Black shale deposition on the northwest African Shelf during the Cenomanian/Turonian oceanic anoxic event: Climate coupling and global organic carbon burial. Paleoceanography PA1006, doi: 10.1029/2003PA000950.

Koutsoukos, E.A.M.,Hart, M.B., 1990. Cretaceous foraminiferal morphogroup distribution patterns, palaeocommunities and trophic structures: a case study from the Sergipe Basin, Brazil. Transact. Roy. Soc. Edinburgh Earth Sci. 81, 221-246.

Koutsoukos, E.A.M., Leary, P.N., Hart, M.B., 1990. Latest Cenomanian - earliest Turonian low-oxygen tolerant benthonic foraminifera: a case study from the Sergipe Basin (N.E.

Brazil) and the western Anglo-Paris Basin (southern England). Palaegeogr., Palaeoclimatol., Palaeoecol. 77, 145-177.

Kuhnt, W., Wiedmann, J., 1995. Cenomanian - Turonian source rocks: paleobiogeographic and paleoenvironmental aspects. In:Huc, A.-Y. (Ed.), Paleogeography, paleoclimate and source rocks. AAPG Studies in Geology, vol. 40, Tulsa, pp. 213-232.

Kuhnt, W., Luderer, F., Nederbragt, S., Thurow, J., Wagner, T., 2005. Orbital-scale record of the late Cenomanian-Turonian oceanic anoxic event (OAE-2) in the Tarfaya Basin (Morocco). Int. J. Earth Sci. (Geol. Rundsch.) 94, 147-159.

Kuypers, M.M.M., Pancost, R.D., Nijenhuis, I.A., Sinninghe Damsté, J.S., 2002. Enhanced productivity led to increased organic carbon burial in the euxinic North Atlantic basin during the late Cenomanian oceanic anoxic event. Paleoceanography 17, PA1051, doi: 10.1029/2000PA000569.

Leary, P.N., Carson, G.A., Cooper, M.K.E., Hart, M.B., Horne, D., Jarvis, I., Rosenfeld, A., Tocher, B.A., 1989. The biotic response to the late Cenomanian oceanic anoxic event; integrated evidence from Dover, SE England. J. Geol. Soc. London 146, 311-317.

Leckie, R.M., 1987. Paleoecology of mid-Cretaceous foraminifera: a comparison of open ocean and epicontinental sea assemblages. Micropaleontol. 33, 164-176.

Leckie, R.M., Yuretich, R.F., West, O.L.O., Finkelstein, D., Schmidt, M., 1998. Paleoceanography of the southwestern Western Interior Sea during the time of the Cenomanian-Turonian boundary (Late Cretaceous). SEPM Concepts Sedimentol. Paleontol. 6, 101-126.

Leckie, R.M., Bralower, T.J., Cashman, R., 2002. Oceanic anoxic events and plankton evolution: biotic response to tectonic forcing during the mid-Cretaceous. Paleoceanography 17, doi: 10.1029/2001PA000623.

MacLeod, K.G., Huber, B.T., Le Ducharme, M., 2000. Paleontological and geochemical constraints on the deep ocean during the Cretaceous greenhouse interval. In: Huber, B.T.,

MacLeod, K.G., Wing, S.L. (Eds.), Warm climates in earth history. Cambridge University Press, Cambridge, pp. 241-274.

Magniez-Jannin, F., 1998. L'élongation des loges chez les foraminifères planctoniques du Crétacé inférieur: une adaptionà la sous-oxygénation des eaux? C. R. Acad. Sci. Serie 2 Sci. Terre Planèt. 326, 207-213.

Mitchell, R.N., Bice, D.M., Montanari, A., Cleaveland, L.C., Christianson, K.T., Ciccioni, R., Hinnov, L.A., 2008. Oceanic anoxic cycles? Orbital prelude to the Bonarelli Level (OAE 2). Earth Planet. Sci. Lett. 267, 1-16.

Mort, H.P., Adatte, T., Föllmi, K.B., Keller, G., Steinmann, P., Matera, V., Berner, Z., Stüben, D., 2007. Phosphorus and the roles of productivity and nutrient recycling during Oceanic Anoxic Event 2. Geology 35, 483-486.

Mort, H.P., Adatte, T., Keller, G., Bartels, D., Föllmi, K.B., Steinmann, P., Berner, Z., Chellai, E.H., 2008. Organic carbon deposition and phosphorus accumulation during Oceanic Anoxic Event 2 in Tarfaya, Morocco. Cret. Res. 29, 1008-1023.

Moy, A.D., Howard, W.R., Bray, S.G., Trull, T.W., 2009. Reduced calcification in modern Southern Ocean planktonic foraminifera. Nature Geosci. 2, 276-280.

Murray, J.W., 1991. Ecology and distribution of planktonic foraminifera. In: Lee J.J., Anderson, O.R. (Eds.), Biology of foraminifera. Academic Press, London, pp. 255-284.

Nederbragt, A.J., 1991. Late Cretaceous biostratigraphy and development of Heterohelicidae (planktic foraminifera). Micropaleontol. 37, 329-372.

Nederbragt, A., Erlich, R.N., Fouke, B.W., Ganssen, G.M., 1998. Palaeoecology of the biserial planktonic foraminifer *Heterohelix moremani* (Cushman) in the late Albian to middle Turonian Circum-North Atlantic. Palaegeogr., Palaeoclimatol., Palaeoecol. 144, 115-133.

Norris, R.D., Wilson, P.A., 1998. Low-latitude sea-surface temperatures for the mid-Cretaceous and the evolution of planktic foraminifera. Geology 26, 823-826.

Norris, R.D., Bice, K.L., Magno, E.A., Wilson, P.A., 2002. Jiggling the thermostat in the Cretaceous hothouse. Geology 30, 299-302.

Ogg, J.G., Agterberg, F.P., Gradstein, F.M., 2004. Cretaceous. In: Gradstein, F.M., Ogg, J.G., Smith, A.G. (Eds.), A geological time scale 2004. Cambridge University Press, Cambridge, pp. 344-383.

Pancost, R.D., Crawford, N., Magness, S., Turner, A., Jenkyns, H.C., Maxwell, J.R., 2004. Further evidence for the development of photic zone euxinic conditions during Mesozoic oceanic anoxic events. J. Geol. Soc. London 161, 353-364.

Parrish, J.T., Curtis, R.L., 1982. Atmospheric circulation, upwelling, and organic-rich rocks in the Mesozoic and Cenozoic Eras. Palaeogeogr., Palaeoclimatol., Palaeoecol. 40, 31-66.

Pavlishina, P.,Wagreich, M., 2009. Palynological investigation of the Cenomanian-Turonian boundary section in the Ultrahelvetic Zone, Eastern Alps, Austria. RECCCE Workshop Gams. Ber. Geol. Bundesanstalt 78, p. 33.

Perch-Nielsen, K., 1985. Mesozoic calcareous nannofossils. In: Bolli, H.M., Saunders, J.B., Perch-Nielsen, K. (Eds.), Plankton Stratigraphy. Cambridge University Press, Cambridge, pp. 329-426.

Poulsen, C.J., Barron, E.J., Johnson, C., Fawcett, P., 1999. Links between climatic factors and regional oceanic circulation in the mid-Cretaceous. GSA Spec. Pap. 332, 73-89.

Poulsen, C.J., Barron, E.J., Arthur, M.A., Peterson, W.H., 2001. Response of the mid-Cretaceous global oceanic circulation to tectonic and $CO_2$ forcings. Paleoceanography 16, 576-592.

Premoli Silva, I., Sliter, W.V., 1999. Cretaceous paleoceanography: Evidence from planktonic foraminiferal evolution. GSA Spec. Pap. 332, 301-328.

1149 Premoli Silva, I., Verga, D., 2004. Practical manual of Cretaceous planktonic foraminifera. In:
1150 Verga, D., Rettori, R. (Eds.), International School on Planktonic Foraminifera, 3° Course:
1151 Cretaceous, 283 pp., Universities of Perugia and Milan, Tipografia Pontefelcina, Perugia.
1152
1153 Premoli Silva, I., Erba, E., Salvini, G., Locatelli, C., Verga, D., 1999. Biotic changes in
1154 Cretaceous Oceanic Anoxic Events of the Tethys. J. Foram. Res. 29, 352-370.
1155
1156 Robaszynski, F., Caron, M., 1995. Foraminifères planctoniques du Crétacé: commentaire de
1157 la zonation Europe-Méditerranée. Bull. Soc. géol. France 166, 681-692.
1158
1159 Sageman, B.B., Meyers,S.R., Arthur, M.A., 2006. Orbital time scale and new C-isotope
1160 record for Cenomanian-Turonian boundary stratotype. Geology 34, 125-128.
1161
1162 Sahagian, D., Pinous, O., Olferiev, A., Zakaharov, V., Beisel, A., 1996. Eustatic curve for the
1163 middle Jurassic – Cretaceous based on Russian platform and Siberian stratigraphy: zonal
1164 resolution. AAPG Bull. 80, 1433-1458.
1165
1166 Schlanger, S.O., Arthur, M.A., Jenkyns, H.C., Scholle, P.A., 1987. The Cenomanian-
1167 Turonian Oceanic Anoxic Event, 1. Stratigraphy and distribution of organic carbon-rich beds
1168 and the marine $\delta^{13}C$ excursion. In: Brooks J., Fleet A.J. (Eds.), Marine Petroleum Source
1169 Rocks. Geol. Soc., London, Spec. Pub., pp. 371-399.
1170
1171 Stampfli, G.M., Borel, G.D., 2002. A plate tectonic model for the Paleozoic and Mesozoic
1172 constrained by dynamic plate boundaries and restored synthetic oceanic isochrones. Earth
1173 Planet. Sci. Let. 196, 17-33.
1174
1175 Strasser, A., Caron, M, Gjermeni, M., 2001. The Aptian, Albian and Cenomanian of Roter
1176 Sattel, Romandes Prealps, Switzerland: a high resolution record of oceanographic changes.
1177 Cret. Res. 22, 173-199.
1178
1179 Tsikos, H., Jenkyns, H.C., Walsworth-Bell, B., Petrizzo, M.R., Forster, A., Kolonic, S., Erba,
1180 E., Premoli-Silva, E., Baas, M. Wagner, T., Sinninghe-Damsté, J.S., 2004. Carbon-Isotope
1181 stratigraphy recorded by the Cenomanian-Turonian Ocenanic Anoxic Event: correlation and
1182 implications based on three key localities. J. Geol. Soc. London 161, 711-719.

van der Zwaan, G.J., Jorissen, F.J., de Stigter, H.C., 1990. The depth dependency of planktonic/benthic foraminiferal ratios: Constraints and applications. Mar. Geol. 95, 1-16.

van der Zwaan, G.J., Duijnstee, I.A.P., den Dulk, M., Ernst, S.R., Jannink, N.T., Kouwenhoven, T.J., 1999. Benthic foraminifers: proxies or problems? A review of paleocological concepts. Earth-Sci. Rev. 46, 213-236.

Wagreich, M., Bojar, A.-V., Sachsenhofer, R.F., Neuhuber, S., Egger, H., 2008. Calcareous nannoplankton, planktonic froraminifera, and carbonate carbon isotope stratigraphy of the Cenomanian-Turonian boundary section in the Ultrahelvetic Zone (Eastern Alps, Upper Austria). Cret. Res. 29, 965-975.

Wan, X., Wignall, P.B., Zhao, W., 2003. The Cenomanian-Turonian extinction and oceanic anoxic event: evidence from southern Tibet. Palaegeogr., Palaeoclimatol., Palaeoecol. 199, 283-298.

West, O.L.O., Leckie, R.M., Schmidt, M., 1998. Foraminiferal paleoecology and paleoceanography of the Greenhorn Cycle along the southwestern margin of the Western Interior Sea. SEPM Concepts Sedimentol. Paleontol. 6, 79-99.

Wilson, P.A., Norris, R.D., Cooper, M.J., 2002. Testing the Cretaceous greenhouse hypothesis using glassy foraminiferal calcite from the core of the Turonian tropics on Demerara Rise. Geology 30, 607-610.

**Figure and Table captions**

Figure 1. Paleogeographical map of the mid-Cretaceous (c. 94 Ma) showing the locations of the investigated section at Rehkogelgraben (1) and important sections referred in the text (2 Pueblo, 3 Eastbourne, 4 Gubbio, 5 Tarfaya, 6 Demerara Rise, 7 Blake Nose). Modified from Kuypers et al. (2002), Gebhardt (1999), Stampfli and Borel (2002). P.O. - Penninic Ocean, W.I.S. – Western Interior Seaway, N.S. – Norwegian Seaway, S.A. – South Atlantic.

Figure 2. Biostratigraphical zonation, carbonate content, $\delta^{13}C$-values of calcareous and organic matter, and sample positions. Calcareous nannoplankton zones, carbonate and $\delta^{13}C_{carb}$-values from Wagreich et al. (2008).

Figure 3. Occurrence of microfossils in thin section. 1) FO of *H.helvetica* based on disaggregated samples, 2) FO of *H.helvetica* based on thin sections.

Figure 4. Chemo- and biostratigraphic correlation between the Cenomanian-Turonian sections at Pueblo (USA, GSSP), Eastbourne (GB), Rehkogelgraben (Austria), and Gubbio (Italy). $\delta^{13}C$-curves from Pueblo, Eastbourne, and Gubbio modified from Tsikos et al. (2004).

Figure 5. Abundances (ind/g) of planktic and benthic foraminifera and of radiolaria.

Figure 6. Planktic foraminiferal species in the Rehkogelgraben-section: 1-3. *Rotalipora cushmani* (sample REH-4/4u), 4-6. *Thalmanninella greenhornensis* (sample RKG-12), 7. *Heterohelix reussi* (sample REH-4/4u), 8-10. *Thalmanninella deekei* (8, 10 sample RKG-03, 9 sample REH-4/4u), 11-13. *Praeglobotruncana gibba* (sample REH-4/4u), 14. *Heterohelix moremani* (sample RKG-12), 15-17. *Praeglobotruncana stephani* (sample REH-4/4u), 18-19. *Dicarinella canaliculata* (sample RKG-07), 20. *Eohastigerinella subdigitata* (sample RKG-06), 21. *Clavihedbergella moremani* (sample RKG-06), 22. *Hedbergella simplex* (sample RKG-12), 23. *Hedbergella delrioensis* (sample RKG-06), 24. *Hedbergella planispira* (sample RKG-12), 25. *Dicarinella imbricata* (sample REH-4/4o), 26-27. *Dicarinella hagni* (sample REH-4/4o), 28-34. *Schackoina cenomana* (28-32 sample RKG-06, 33, 34 sample RKG-08a, 30-32 unusual morphotypes), 35-37. *Whiteinella archaeocretacea* (sample RKG-09), 38-40. *Whiteinella baltica* (sample RKG-12), 41. *Gümbelitria cenomana* (sample RKG-08a), 42-44. *Whiteinella brittonensis* (sample RKG-12), 45-46. *Helvetoglobotruncana helvetica* (sample RKG-10), 47. *Marginulina* sp. cf. *M. renzi* (sample RKG-11). Length of scale bars: 0.1 mm.

Figure 7. Distribution of *K*-strategist planktonic foraminifera (equilibrium species) and intermediate species. Note that percentages (open circles) are displayed always with the same scale, while inividuals per gram sediment (black diamonds) are displayed on different scales. A: Rotaliporids, B: *Praeglobotruncana* spp., C: *Dicarinella* spp., D. *Whiteinella* spp.

Figure 8. Distribution of *r*-strategist planktonic foraminifera (potential opportunists) and intermediate species. Note that percentages (open circles) are displayed always with the same scale, while inividuals per gram sediment (black diamonds) are displayed on different scales. A: *Hedbergella* spp., B: *Schackoina cenomana*, C: *Heterohelix* spp., D. *Gümbelitria cenomana*.

Figure 9. Arenaceous/calcareous benthic foraminifera ratio and distribution (ind/g) of benthic morphogroups.

Figure 10. Benthic foraminiferal species in the Rehkogelgraben-section: 1. *Ammobaculites* cf. *amabilis* (sample REH-4/2b), 2. *Ammobaculites fragmentarius* (sample RKG-03), 3. *Ammobaculites subcretacea* (sample REH-4/4u), 4. *Ammobaculoides mosbyensis* (sample RKG-04), 5. *Ammodiscus cretaceus* (sample RKG-12), 6. *Ammomarginulina lorangerae* (sample RKG-08a), 7. *Ammosphaeroidina sphaeroidiniformis* (sample RKG-08a), 8. *Bathysiphon* sp. (sample REH-4/4o), 9. *Bulbobaculites problematicus* (sample RKG-10), 10. *Haplophragmoides excavatus* (sample RKG-15), 11. *Haplophragmoides rugosa* (sample RKG-05), 12. *Haplophragmoides* sp. cf. *H. walteri* (sample RKG-10), 13. *Haplophragmium* sp. (sample RKG-05), 14. *Hyperammina gaultina* (sample RKG-06), 15. *Kalamopsis* sp. (sample RKG-12), 16. *Marssonella oxycona* (sample RKG-12), 17. ?*Martinottiella* sp. (sample RKG-12), 18. *Plectina pinswangensis* (sample RKG-04), 19. *Psammosphaera fusca* (sample REH-2/32), 20. *Recurvoides* sp. (sample RKG-06), 21. *Reophax minuta* (sample RKG-07), 22. *Reophax splendida* (sample RKG-07), 23. *Saccammina alexanderi* (sample REH-4/4o), 24. *Saccammina globosa* (sample RKG-01), 25. *Spiroplectammina roemeri* (sample REH-4/2b), 26. *Tritaxia gaultina* (sample RKG-12), 27. *Trochammina* sp. cf. *T. depressa* (sample REH-4/4o), 28. *Trochammina umiatensis* (sample RKG-06), 29. *Trochamminoides variolarius* (sample RKG-12), 30. *Trochamminoides* sp. (sample RKG-12), 31. *Verneuilina münsteri* (sample RKG-01), 32. *Bolivina anambra* (sample REH-4/2b), 33. *Bolivina* sp. cf. *B. incrassata* (sample RKG-04), 34. *Cibicides beaumontianus* (sample RKG-06), 35. *Dentalina catenula* (sample RKG-02), 36. *Dentalina marginuloides* (sample REH-4/2b), 37. *Eouvigerina cretae* (sample REH-4/1), 38. *Eouvigerina* sp. (sample RKG-14), 39. *Gabonita* sp. cf. *G. ogugensis* (sample RKG-02), 40. *Berthelina dakotensis* (sample RKG-12), 41. *Gavelinella* sp. (sample RKG-14), 42. *Gavelinella* sp. (sample RKG-02), 43. *Gyroidinoides lenticulus* (sample RKG-05), 44. *Gyroidinoides umbilicatus* (sample RKG-12), 45. *Lenticulina exarata* (sample RKG-02), 46. *Lenticulina gaultina* (sample REH-4/2b), 47.

*Lenticulina marcki* (sample REH-4/2b), 48. *Lenticulina pulchella* (sample RKG-06), 49. *Lenticulina saxocretace*a (sample REH-4/4o), 50. *Neobulimina albertensis* (sample RKG-12), 51. *Nodosaria* sp. (sample RKG-12), 52. *Nonionella* cf. *robusta* (sample REH-4/4o), 53. *Osangularia cordieriana* (sample RKG-02), 54. *Osangularia* sp. (sample REH-2/32), 55. *Planularia complanata* (sample RKG-09), 56. *Planularia dissona* (sample REH-4/2b), 57. *Planularia* sp. cf. *P. umbonata* (sample RKG-02), 58. *Planulina stelligera* (sample RKG-06), 59. *Planulina texana* Cushman (sample REH-4/2b), 60. *Pleurostomella subnodosa* (sample RKG-11), 61. *Praebulimina* sp. (sample RKG-08a), 62. *Praebulimina robusta* (sample RKG-07), 63. *Praebulimina ventricosa* (sample RKG-02), 64. *Pullenia minuta* (sample RKG-03), 65. *Pullenia reussi* (sample RKG-03), 66. *Ramulina aculeata* (sample RKG-03), 67. *Rotalia polyrraphes* (sample REH-4/4u), 68. *Scheibnerova* sp. (sample RKG-03), 69. *Tappanina laciniosa* (sample RKG-12). Length of scale bars: 0.1 mm.

Figure 11. Benthic foraminiferal size-trends and interpretation. Closed circles indicate frequency of large specimens >0.250 mm, open circles for specimens of 0.125 to 0.250 mm, and black diamonds for small specimens from 0.063 to 0.125 mm. Absence of symbols indicates absence of specimens in the sample. Note the logarithmic scale.

Figure 12. Frequency of planktic foraminiferal genera during the Cenomanian-Turonian boundary interval and simple diversity (number of taxa) of planktic and benthic foraminifera. Key to genera: closely dotted line - *Gümbelitria*, narrowly dashed line with open circles - *Schackoina*, poin-dash line with open circles - *Heterohelix*, double pointed line - *Praeglobotruncana*, widely dashed line - *Whiteinella*, continuous line - *Hedbergella*.

Table 1. Distribution of planktic foraminifera picked. Data for sample REH 4/1 are displayed in italics because of the allochthone orign of the specimens.

Table 2. Distribution of benthic foraminifera picked. Data for sample REH 4/1 are displayed in italics because of the allochthone orign of the specimens.

Table 3. Distribution of radiolaria picked.

Table 4. $\delta^{13}C_{org}$ and abundances of planktic and benthic foraminifera and of radiolaria.

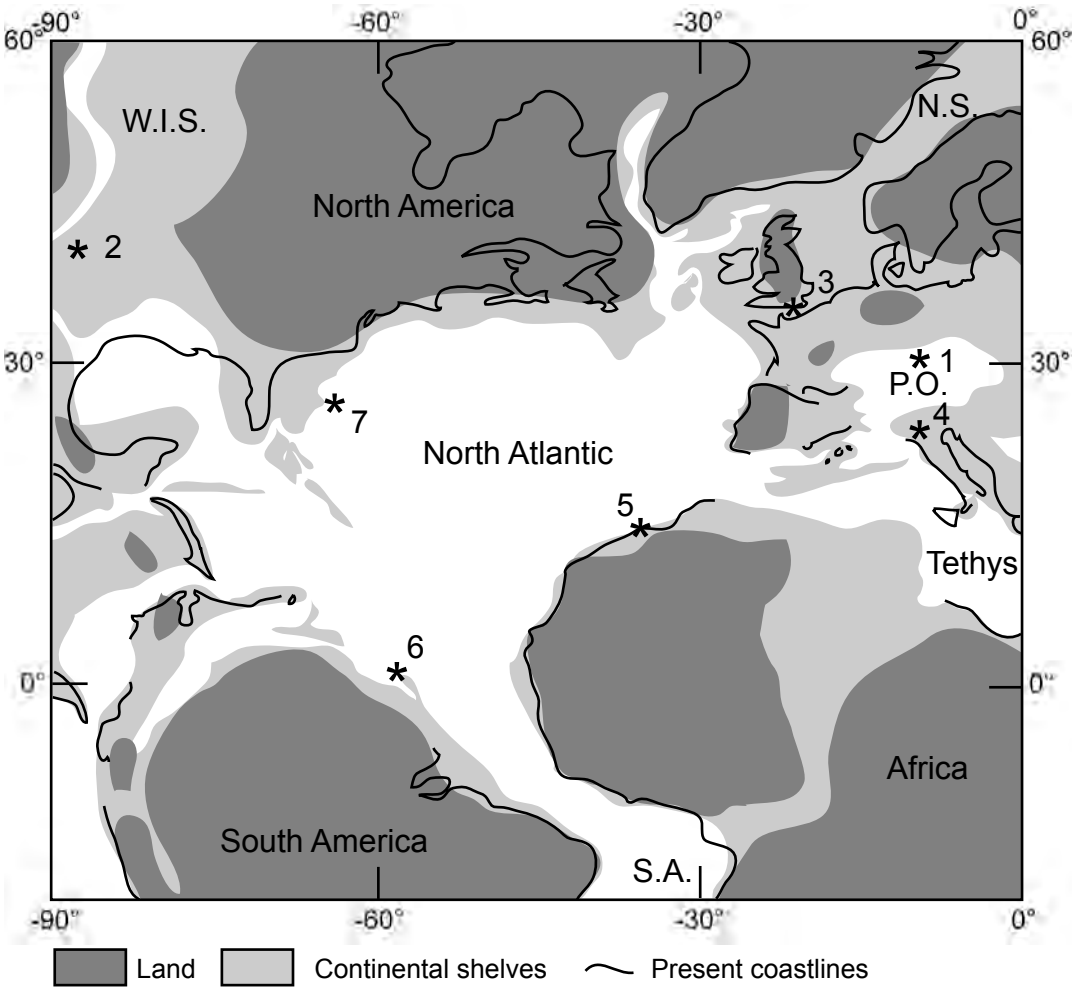
-90°
-60°
-30°
0°
60°
30°
0°
W.I.S.
North America
N.S.
2
3
1
P.O.
4
7
North Atlantic
5
Tethys
6
Africa
South America
S.A.
Land
Continental shelves
Present coastlines

Late Cenomanian
Early Turonian
CC 10
CC 11
UC 4
UC 5-6
UC 7
R. cushmani
W. archaeocretacea
H. helvetica
Nannofoss. biostrat.
Planktic foram. zones
Lithology
Foraminifral index species
Samples (this paper)
FO H. helvetica
LO Rotalipora spp.
RKG-11
RKG-10
RKG-09
RKG-08
REH2/34c
RKG-07
RKG-06
REH2/32
REH2/31
REH2/31m
RKG-15
REH4/1
RKG-14
REH2/30B2
REH2/30B1-
RKG-05
REH4/2b
RKG-04
REH4/4o
REH4/4u
RKG-03
RKG-12
RKG-02
RKG-01
CaCO3
δ13Ccarb
δ13Corg
m
0
50
100 %
2
3
4 ‰
-28
-27
-26
-25
-24
-23 ‰

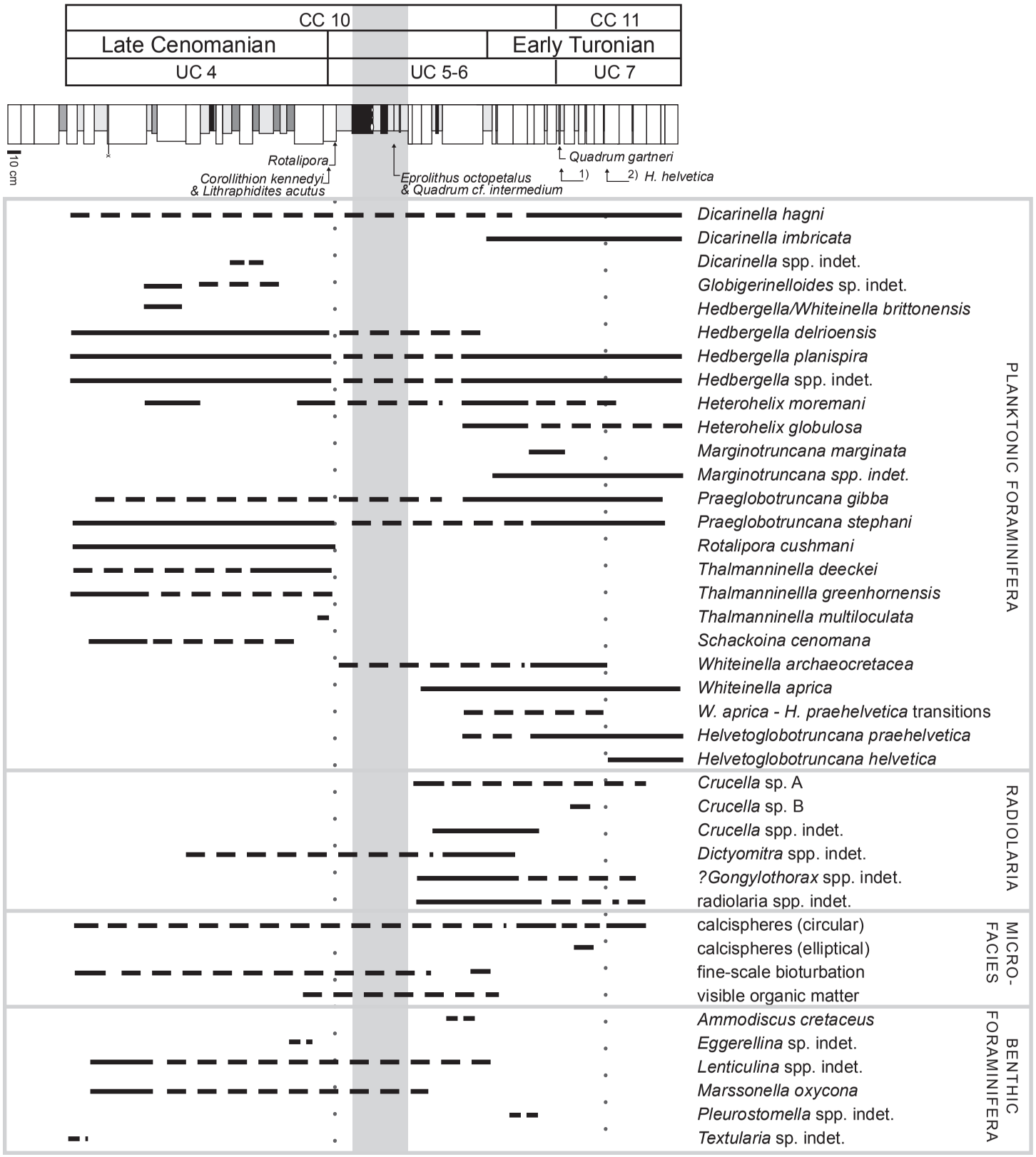
CC 10
CC 11
Late Cenomanian
Early Turonian
UC 4
UC 5-6
UC 7
10 cm
Rotalipora
Corollithion kennedyi
& Lithraphidites acutus
Eprolithus octopetalus
& Quadrum cf. intermedium
Quadrum gartneri
1)
2) H. helvetica
Dicarinella hagni
Dicarinella imbricata
Dicarinella spp. indet.
Globigerinelloides sp. indet.
Hedbergella/Whiteinella brittonensis
Hedbergella delrioensis
Hedbergella planispira
Hedbergella spp. indet.
Heterohelix moremani
Heterohelix globulosa
Marginotruncana marginata
Marginotruncana spp. indet.
Praeglobotruncana gibba
Praeglobotruncana stephani
Rotalipora cushmani
Thalmanninella deeckei
Thalmanninellla greenhornensis
Thalmanninella multiloculata
Schackoina cenomana
Whiteinella archaeocretacea
Whiteinella aprica
W. aprica - H. praehelvetica transitions
Helvetoglobotruncana praehelvetica
Helvetoglobotruncana helvetica
PLANKTONIC FORAMINIFERA
Crucella sp. A
Crucella sp. B
Crucella spp. indet.
Dictyomitra spp. indet.
?Gongylothorax spp. indet.
radiolaria spp. indet.
RADIOLARIA
calcispheres (circular)
calcispheres (elliptical)
fine-scale bioturbation
visible organic matter
MICRO-FACIES
Ammodiscus cretaceus
Eggerellina sp. indet.
Lenticulina spp. indet.
Marssonella oxycona
Pleurostomella spp. indet.
Textularia sp. indet.
BENTHIC FORAMINIFERA
Rotalipora cushmani Zone
W. archaeocretacea Zone
H. helvetica Zone
?

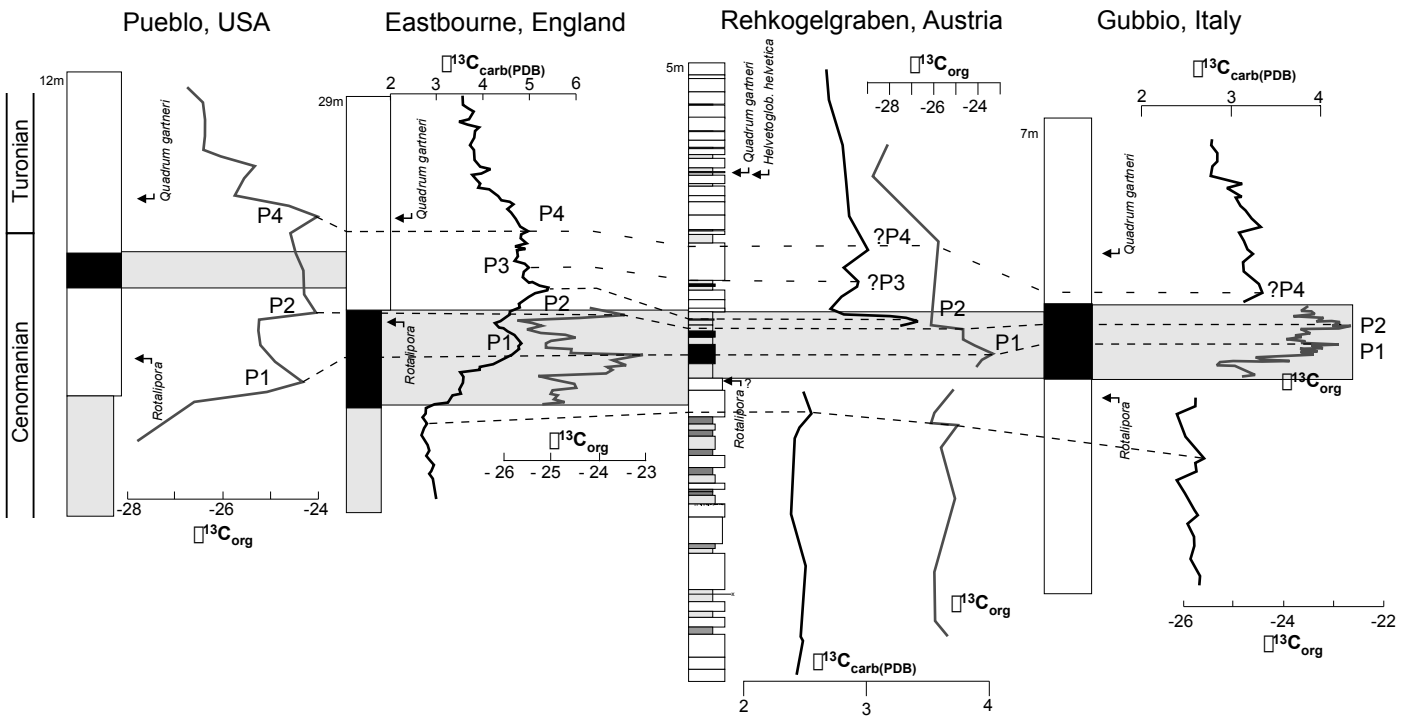
Pueblo, USA
Eastbourne, England
Rehkogelgraben, Austria
Gubbio, Italy
Turonian
Cenomanian
12m
29m
5m
7m
Quadrum gartneri
Helvetoglob. helvetica
Rotalipora
P1
P2
P3
P4
?P3
?P4
-28
-26
-24
-25
-23
-22
2
3
4
5
6

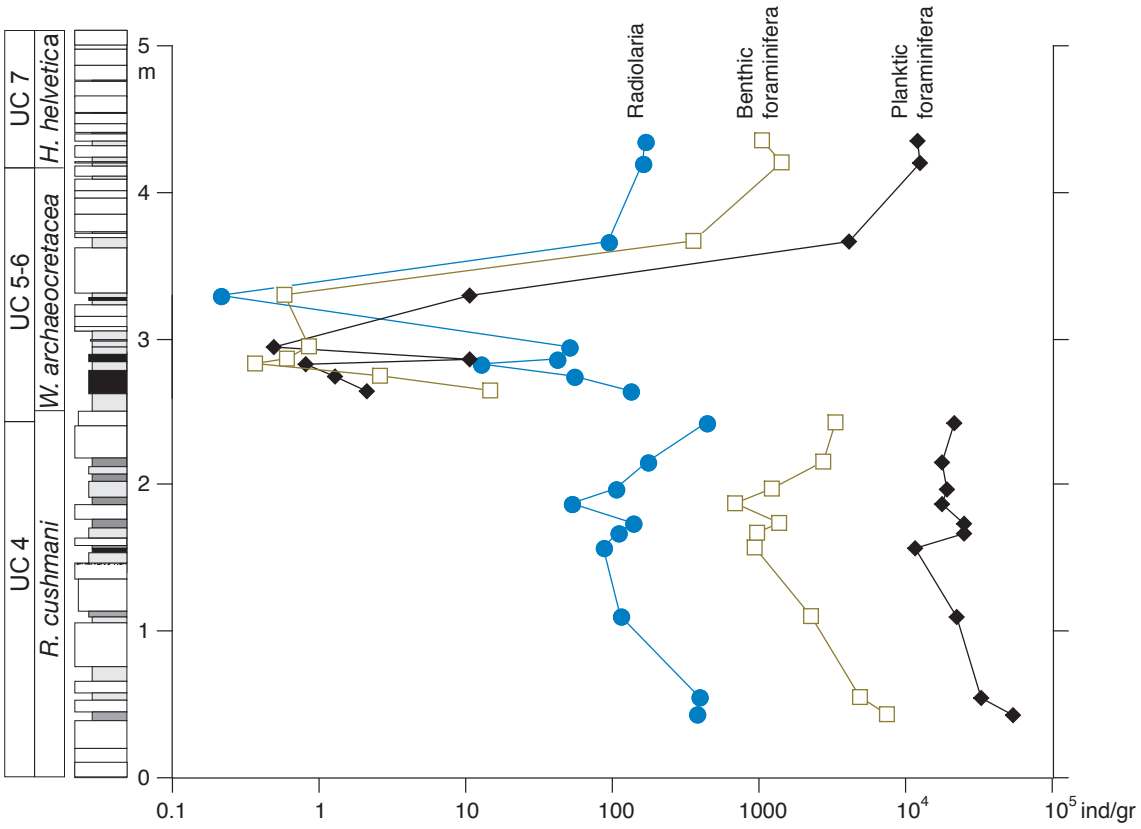
UC 7
H. helvetica
UC 5-6
W. archaeocretacea
UC 4
R. cushmani
5
m
4
3
2
1
0
Radiolaria
Benthic foraminifera
Planktic foraminifera
0.1
1
10
100
1000
10^4
10^5 ind/gr

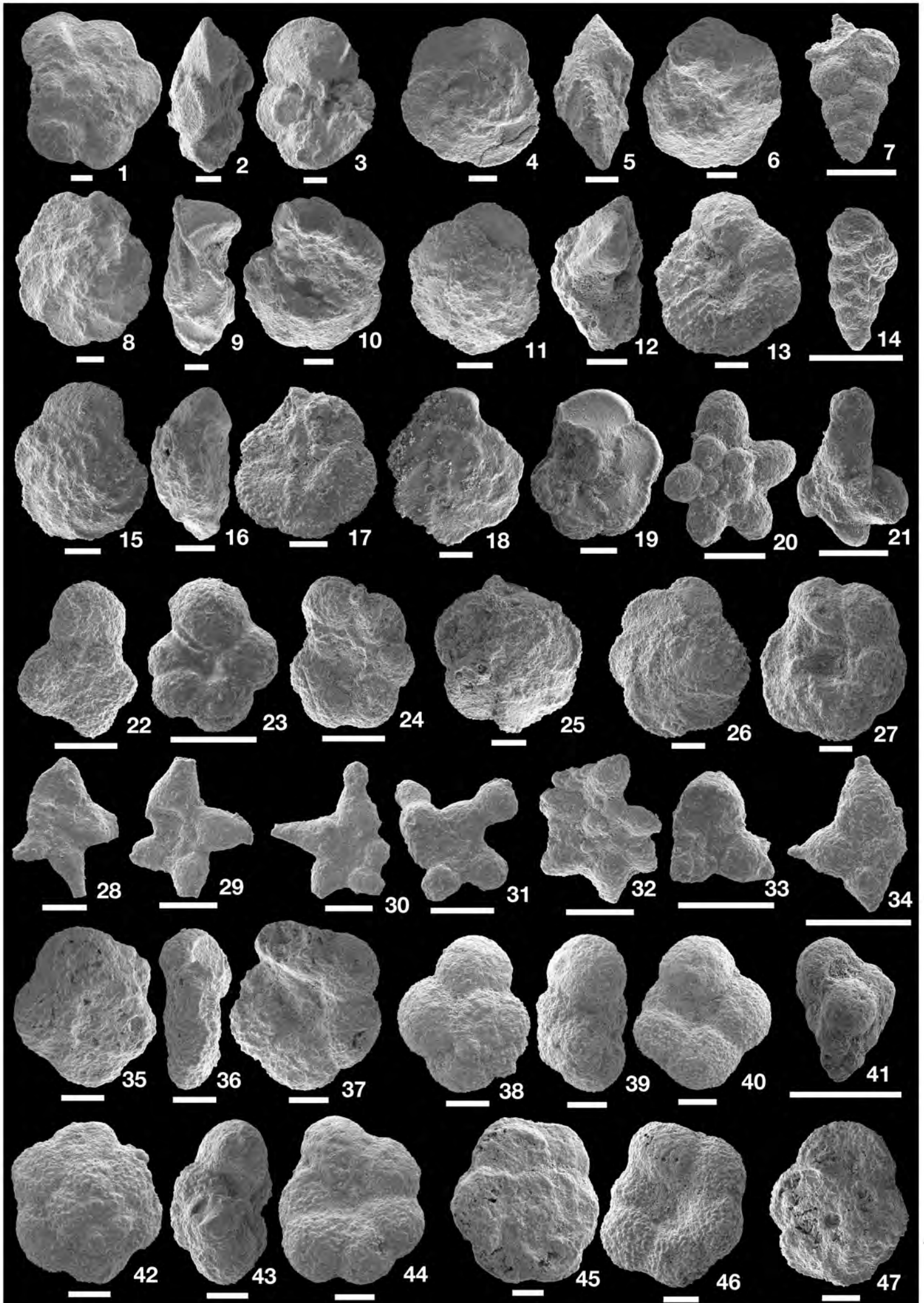
1
2
3
4
5
6
7
8
9
10
11
12
13
14
15
16
17
18
19
20
21
22
23
24
25
26
27
28
29
30
31
32
33
34
35
36
37
38
39
40
41
42
43
44
45
46
47

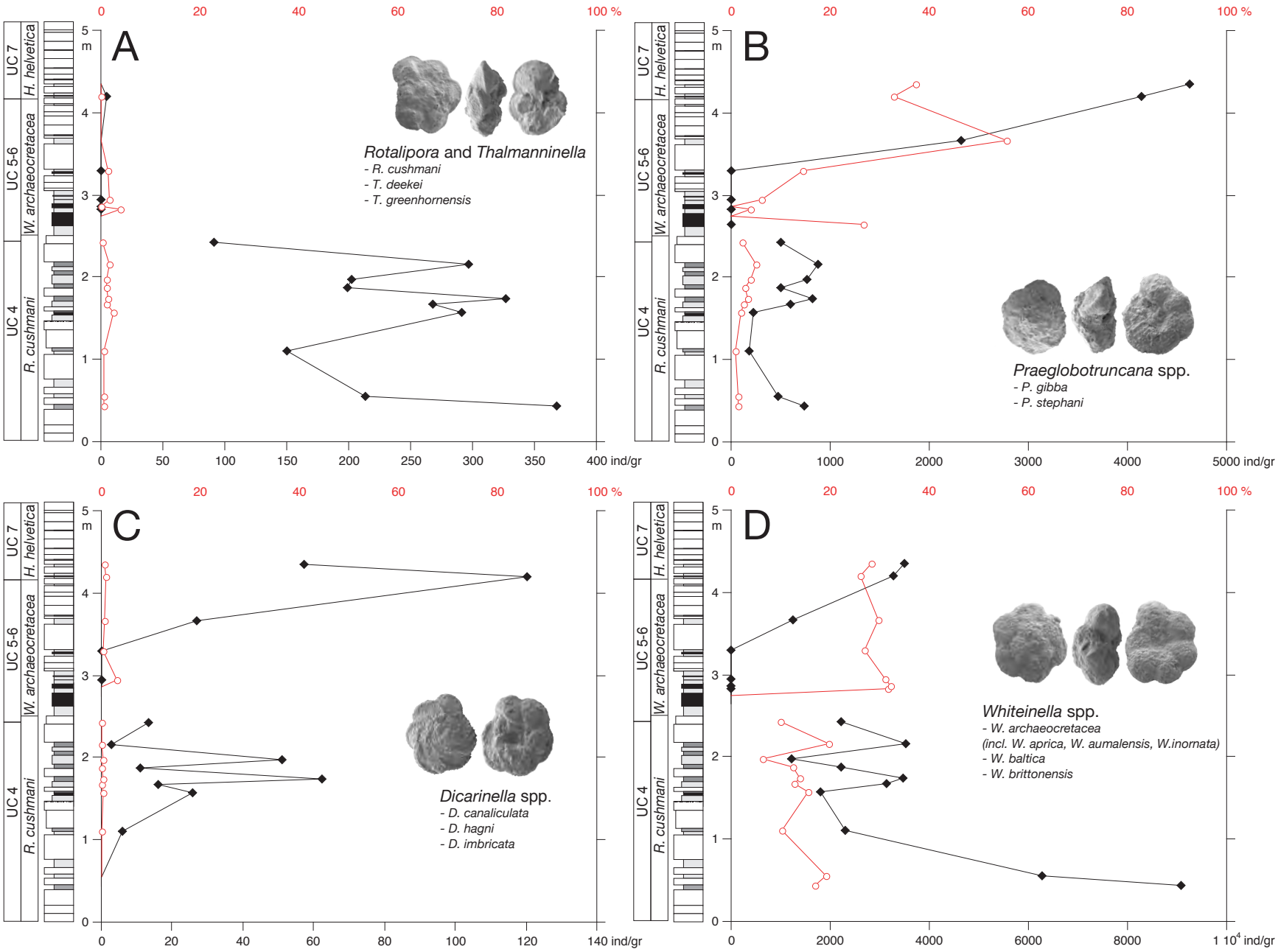
A
B
C
D
UC 7
H. helvetica
UC 5-6
W. archaeocretacea
UC 4
R. cushmani
m
0 20 40 60 80 100 %
0 50 100 150 200 250 300 350 400 ind/gr
0 1000 2000 3000 4000 5000 ind/gr
0 20 40 60 80 100 120 140 ind/gr
0 2000 4000 6000 8000 1 10^4 ind/gr
Rotalipora and Thalmanninella
- R. cushmani
- T. deekei
- T. greenhornensis
Praeglobotruncana spp.
- P. gibba
- P. stephani
Dicarinella spp.
- D. canaliculata
- D. hagni
- D. imbricata
Whiteinella spp.
- W. archaeocretacea
(incl. W. aprica, W. aumalensis, W.inornata)
- W. baltica
- W. brittonensis

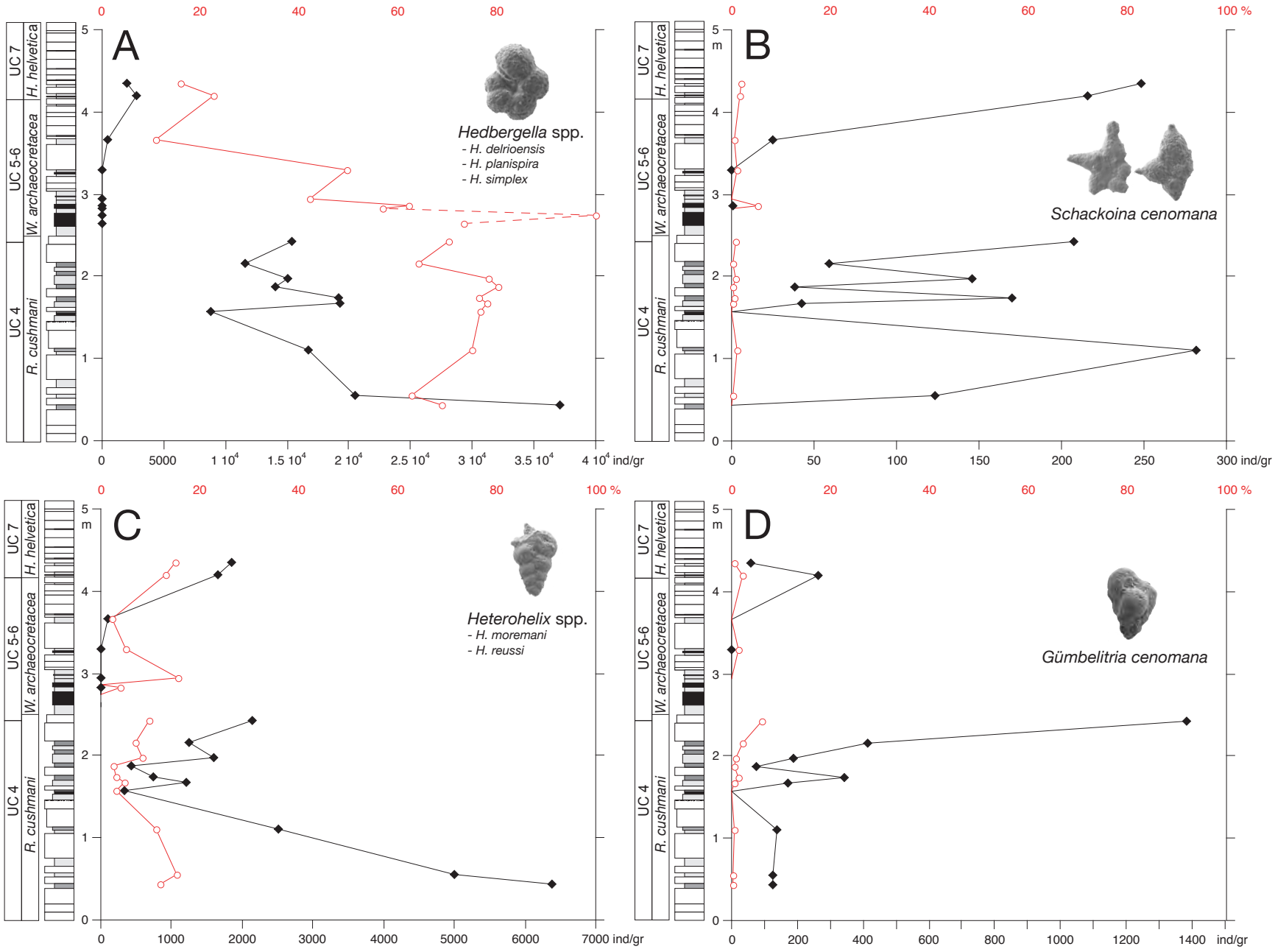
A
B
C
D
UC 7
H. helvetica
UC 5-6
W. archaeocretacea
UC 4
R. cushmani
m
Hedbergella spp.
- H. delrioensis
- H. planispira
- H. simplex
Schackoina cenomana
Heterohelix spp.
- H. moremani
- H. reussi
Gümbelitria cenomana
0 20 40 60 80 100 %
0 5000 1 10^4 1.5 10^4 2 10^4 2.5 10^4 3 10^4 3.5 10^4 4 10^4 ind/gr
0 50 100 150 200 250 300 ind/gr
0 1000 2000 3000 4000 5000 6000 7000 ind/gr
0 200 400 600 800 1000 1200 1400 ind/gr

UC 4
UC 5-6
UC 7
R. cushmani
W. archaeocretacea
H. helvetica
arenaceous species
calcareous species
m
0
1
2
3
4
5
0 20 40 60 80 100
%
Ammobaculites spp.
Bathysiphon spp.
Haplophragmoides spp.
Reophax spp.
Spiroplectammina spp.
Tritaxia sp.
Trochammina spp.
other arenaceous species
0 500
ind/gr
Turrilinids
0 1000
ind/gr
Gavelinellids spp. and
Planulina spp.
elongated Nodosariids
Gyroidinoides
0 1000
ind/gr
lensiform Nodosariids
Gabonita sp.
2000 3000
Bolivina spp.
other calcareous species
4000
ind/gr

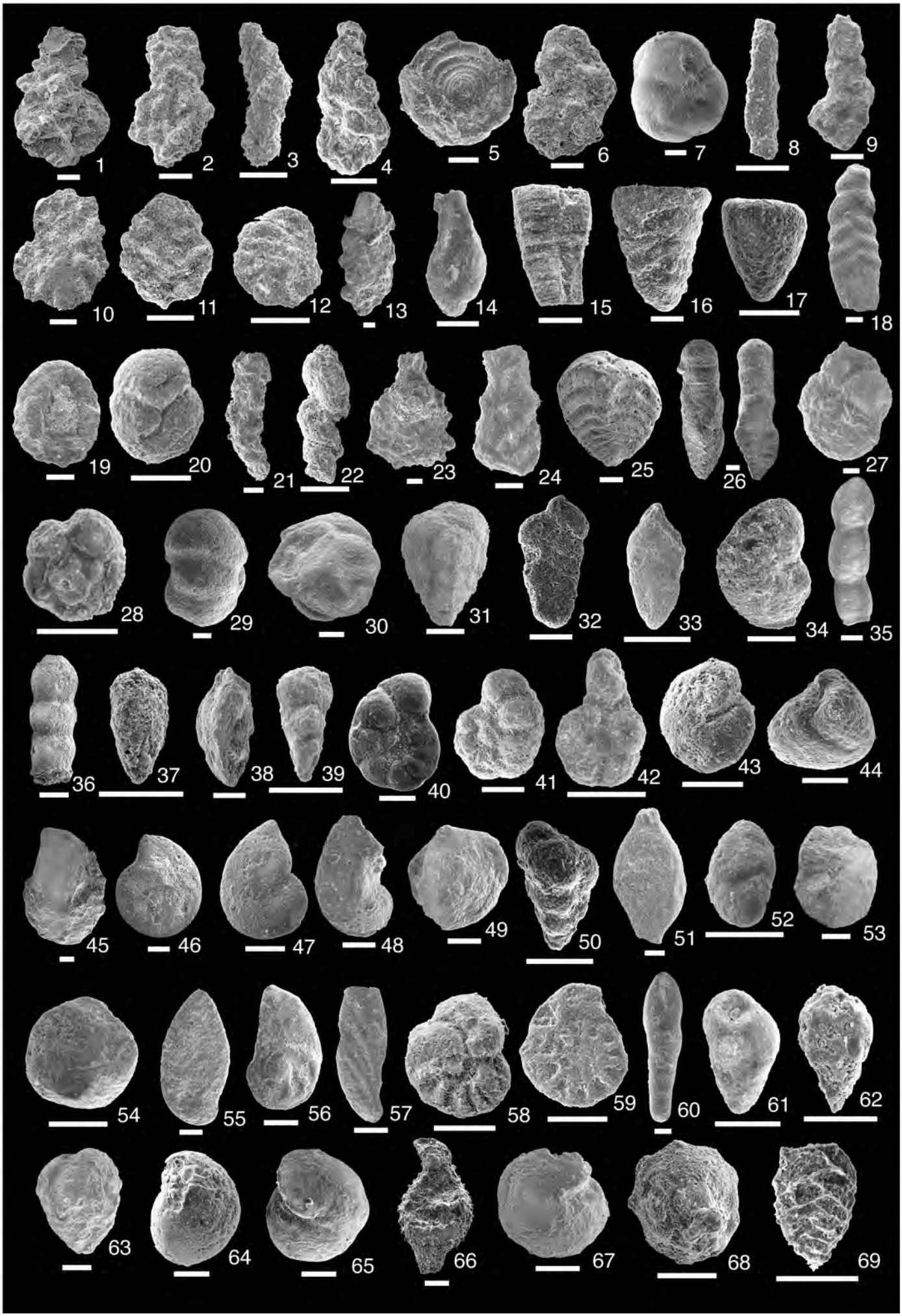
1
2
3
4
5
6
7
8
9
10
11
12
13
14
15
16
17
18
19
20
21
22
23
24
25
26
27
28
29
30
31
32
33
34
35
36
37
38
39
40
41
42
43
44
45
46
47
48
49
50
51
52
53
54
55
56
57
58
59
60
61
62
63
64
65
66
67
68
69

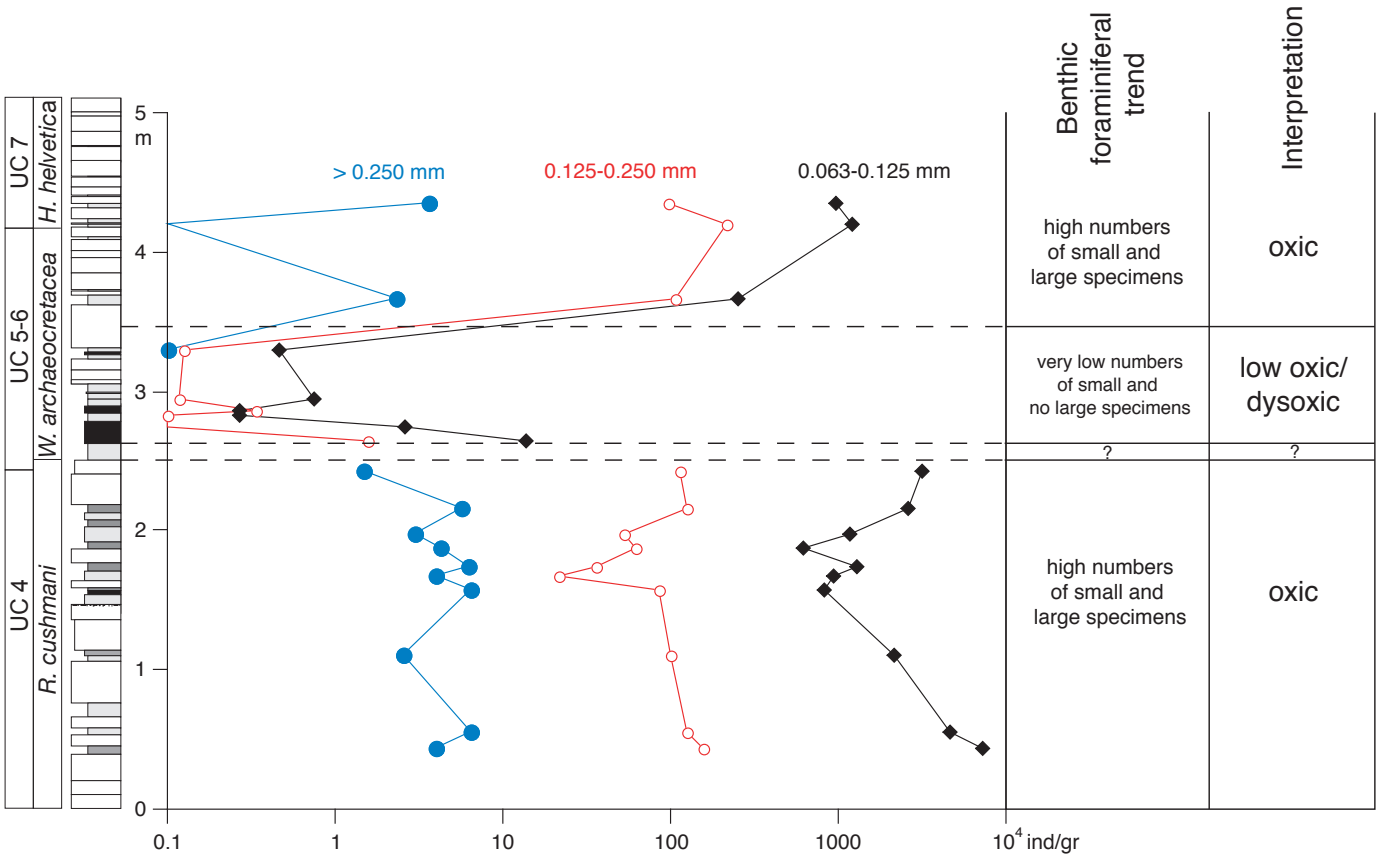
UC 7
H. helvetica
UC 5-6
W. archaeocretacea
UC 4
R. cushmani
5
m
4
3
2
1
0
> 0.250 mm
0.125-0.250 mm
0.063-0.125 mm
0.1
1
10
100
1000
10^4 ind/gr
Benthic foraminiferal trend
Interpretation
high numbers of small and large specimens
oxic
very low numbers of small and no large specimens
low oxic/ dysoxic
?
?
high numbers of small and large specimens
oxic

UC 4
R. cushmani
UC 5-6
W. archaeocretacea
UC 7
H. helvetica
Gümbelitria
Schackoina
Heterohelix
Praeglobotruncana
Whiteinella
Hedbergella
3.5
3.4
3.3
3.2
3.1
3
2.9
2.8
2.7
2.6
0
1
2
3
4
5
6
ind/gr 7
Planktic taxa
Benthic taxa
0
5
10 no. of taxa 15

**A: Fraction >0.250 mm**

| Sample | Split | *D. canaliculata* | *D. hagni* | *D. imbricata* | *H. helvetica* | *M. cf. renzi* | *P. gibba* | *P. stephani* | *R. cushmani* | *T. greenhornensis* | *T. deeckei* | *W. baltica* | *W. brittonensis* | *W. archaeocretacea* |
|---|---|---|---|---|---|---|---|---|---|---|---|---|---|---|
| RKG-01 | 128 | 0 | 0 | 0 | 0 | 0 | 16 | 30 | 305 | 3 | 0 | 2 | 0 | 0 |
| RKG-02 | 64 | 0 | 0 | 0 | 0 | 0 | 16 | 50 | 420 | 14 | 8 | 6 | 0 | 0 |
| RKG-12 | 64 | 0 | 0 | 0 | 0 | 0 | 14 | 29 | 277 | 58 | 8 | 46 | 21 | 0 |
| RKG-03 | 128 | 0 | 4 | 0 | 0 | 0 | 26 | 52 | 334 | 19 | 25 | 8 | 6 | 0 |
| REH 4/4 u | 128 | 0 | 8 | 0 | 0 | 0 | 74 | 84 | 259 | 17 | 13 | 12 | 4 | 0 |
| REH 4/4 o | 32 | 0 | 13 | 9 | 0 | 0 | 100 | 85 | 195 | 21 | 16 | 3 | 3 | 0 |
| REH 4/2b | 64 | 0 | 0 | 2 | 0 | 0 | 106 | 49 | 228 | 17 | 5 | 0 | 0 | 0 |
| RKG-04 | 128 | 0 | 2 | 4 | 0 | 0 | 157 | 93 | 179 | 11 | 0 | 0 | 0 | 0 |
| RKG-05 | 64 | 0 | 0 | 3 | 0 | 0 | 74 | 83 | 228 | 12 | 1 | 3 | 0 | 0 |
| RKG-14 | 32 | 0 | 2 | 2 | 0 | 0 | 119 | 89 | 119 | 36 | 12 | 34 | 32 | 24 |
| *REH 4/1* | *1* | *0* | *0* | *2* | *0* | *0* | *21* | *16* | *207* | *32* | *9* | *0* | *0* | *0* |
| RKG-15 | 1 | 0 | 0 | 0 | 0 | 0 | 3 | 0 | 0 | 0 | 0 | 0 | 0 | 0 |
| REH 2/31 | 8 | 0 | 0 | 0 | 0 | 0 | 0 | 0 | 0 | 0 | 0 | 0 | 0 | 0 |
| REH 2/32 | 1 | 0 | 0 | 0 | 0 | 0 | 0 | 1 | 3 | 0 | 0 | 0 | 0 | 0 |
| RKG-06 | 1 | 0 | 0 | 0 | 0 | 0 | 0 | 0 | 0 | 0 | 0 | 0 | 0 | 0 |
| RKG-07 | 1 | 3 | 0 | 1 | 0 | 0 | 2 | 0 | 0 | 0 | 0 | 0 | 0 | 0 |
| RKG-08 | 1 | 0 | 2 | 0 | 0 | 0 | 4 | 1 | 10 | 2 | 0 | 0 | 0 | 5 |
| RKG-09 | 512 | 0 | 3 | 0 | 0 | 0 | 280 | 102 | 0 | 0 | 0 | 17 | 21 | 183 |
| RKG-10 | 128 | 0 | 28 | 4 | 15 | 0 | 284 | 175 | 0 | 3 | 0 | 17 | 9 | 78 |
| RKG-11 | 256 | 0 | 16 | 0 | 11 | 4 | 337 | 168 | 0 | 0 | 0 | 18 | 13 | 107 |

**B: Fraction 0.125-0.250 mm**

| Sample | Split | *C. moremani* | *D. canaliculata* | *D. hagni* | *D. imbricata* | *E. subdigitata* | *H. delrioensis* | *H. planispira* | *H. simplex* | *H. moremani* | *H. reussi* | *P. gibba* | *P. stephani* | *R. cushmani* | *S. cenomana* | *T. greenhornensis* | *T. deekei* | *W. archaeocretacea* | *W. baltica* | *W. brittonensis* |
|---|---|---|---|---|---|---|---|---|---|---|---|---|---|---|---|---|---|---|---|---|
| RKG-01 | 1024 | 0 | 0 | 0 | 0 | 0 | 53 | 25 | 30 | 2 | 3 | 21 | 35 | 7 | 0 | 1 | 0 | 79 | 13 | 1 |
| RKG-02 | 1024 | 0 | 0 | 0 | 0 | 0 | 53 | 21 | 23 | 6 | 7 | 14 | 27 | 0 | 0 | 0 | 0 | 90 | 15 | 2 |
| RKG-12 | 512 | 0 | 0 | 2 | 0 | 0 | 214 | 80 | 66 | 0 | 1 | 25 | 32 | 6 | 1 | 3 | 0 | 75 | 41 | 12 |
| RKG-03 | 1024 | 0 | 0 | 4 | 1 | 0 | 79 | 25 | 20 | 0 | 0 | 11 | 27 | 4 | 0 | 11 | 0 | 39 | 13 | 2 |
| REH 4/4 u | 1024 | 0 | 0 | 1 | 1 | 0 | 271 | 41 | 24 | 0 | 0 | 39 | 54 | 6 | 0 | 8 | 0 | 61 | 17 | 9 |
| REH 4/4 o | 256 | 0 | 0 | 6 | 0 | 0 | 96 | 34 | 26 | 0 | 0 | 37 | 56 | 7 | 0 | 2 | 8 | 24 | 14 | 5 |
| REH 4/2b | 512 | 0 | 0 | 1 | 1 | 0 | 85 | 15 | 15 | 0 | 0 | 43 | 42 | 6 | 0 | 4 | 0 | 31 | 4 | 0 |
| RKG-04 | 1024 | 0 | 0 | 6 | 2 | 0 | 130 | 42 | 30 | 0 | 0 | 58 | 41 | 9 | 1 | 2 | 0 | 57 | 18 | 0 |
| RKG-05 | 512 | 0 | 0 | 0 | 0 | 1 | 142 | 23 | 31 | 0 | 0 | 66 | 33 | 8 | 0 | 2 | 0 | 49 | 35 | 1 |
| RKG-14 | 512 | 0 | 0 | 2 | 0 | 0 | 141 | 18 | 24 | 0 | 0 | 19 | 37 | 2 | 3 | 3 | 0 | 15 | 63 | 11 |
| *REH 4/1* | *8* | *0* | *1* | *1* | *0* | *0* | *12* | *3* | *0* | *0* | *0* | *33* | *53* | *3* | *0* | *16* | *0* | *33* | *8* | *7* |
| RKG-15 | 32 | 0 | 0 | 0 | 0 | 0 | 1 | 0 | 0 | 0 | 0 | 0 | 1 | 0 | 0 | 0 | 0 | 0 | 0 | 0 |
| REH 2/31 | 128 | 0 | 0 | 0 | 0 | 0 | 0 | 0 | 0 | 0 | 0 | 0 | 0 | 0 | 0 | 0 | 0 | 0 | 0 | 0 |
| REH 2/32 | 1 | 0 | 0 | 0 | 0 | 0 | 12 | 2 | 1 | 0 | 0 | 0 | 2 | 0 | 0 | 0 | 0 | 0 | 0 | 0 |
| RKG-06 | 2 | 1 | 0 | 0 | 0 | 3 | 254 | 8 | 28 | 0 | 0 | 0 | 0 | 1 | 20 | 0 | 0 | 6 | 9 | 0 |
| RKG-07 | 2 | 0 | 0 | 0 | 0 | 0 | 3 | 0 | 0 | 0 | 0 | 1 | 0 | 1 | 0 | 0 | 0 | 2 | 4 | 0 |
| RKG-08 | 1 | 0 | 0 | 0 | 1 | 0 | 127 | 26 | 18 | 0 | 0 | 32 | 130 | 1 | 0 | 3 | 0 | 29 | 10 | 5 |
| RKG-09 | 4096 | 0 | 0 | 4 | 0 | 0 | 33 | 9 | 0 | 0 | 0 | 62 | 203 | 0 | 0 | 0 | 0 | 36 | 16 | 4 |
| RKG-10 | 1024 | 0 | 0 | 4 | 2 | 0 | 84 | 23 | 13 | 0 | 0 | 75 | 140 | 0 | 0 | 0 | 0 | 42 | 25 | 0 |
| RKG-11 | 2048 | 0 | 0 | 4 | 0 | 0 | 48 | 19 | 16 | 1 | 1 | 153 | 186 | 0 | 0 | 0 | 0 | 39 | 19 | 0 |

**C: Fraction 0.063-0.125 mm**

| Sample | Split | *G. cenomana* | *H. delrioensis* | *H. planispira* | *H. simplex* | *H. moremani* | *H. reussi* | *P. gibba* | *P. stephani* | *S. cemonana* | *W. archaeocretacea* | *W. baltica* | *W. brittonensis* |
|---|---|---|---|---|---|---|---|---|---|---|---|---|---|
| RKG-01 | 16384 | 1 | 223 | 47 | 15 | 22 | 28 | 1 | 1 | 0 | 54 | 12 | 0 |
| RKG-02 | 8192 | 2 | 261 | 39 | 19 | 41 | 38 | 2 | 0 | 2 | 74 | 14 | 0 |
| RKG-12 | 8192 | 3 | 255 | 66 | 16 | 34 | 20 | 0 | 0 | 6 | 28 | 13 | 0 |
| RKG-03 | 8192 | 0 | 162 | 47 | 10 | 8 | 1 | 0 | 0 | 0 | 32 | 9 | 0 |
| REH 4/4 u | 8192 | 4 | 333 | 61 | 13 | 18 | 10 | 0 | 0 | 1 | 41 | 21 | 0 |
| REH 4/4 o | 2048 | 6 | 269 | 40 | 9 | 8 | 5 | 0 | 0 | 3 | 37 | 19 | 0 |
| REH 4/2b | 4096 | 2 | 296 | 45 | 9 | 7 | 4 | 0 | 0 | 1 | 38 | 15 | 0 |
| RKG-04 | 8192 | 4 | 251 | 36 | 8 | 22 | 12 | 0 | 0 | 3 | 10 | 7 | 0 |
| RKG-05 | 4096 | 7 | 143 | 26 | 1 | 13 | 8 | 0 | 0 | 1 | 35 | 14 | 0 |
| RKG-14 | 4096 | 29 | 243 | 49 | 9 | 27 | 18 | 0 | 2 | 4 | 7 | 28 | 0 |
| *REH 4/1* | *64* | *1* | *19* | *8* | *0* | *0* | *3* | *0* | *0* | *0* | *18* | *6* | *0* |
| RKG-15 | 64 | 0 | 1 | 0 | 0 | 0 | 0 | 0 | 0 | 0 | 0 | 0 | 0 |
| REH 2/31 | 256 | 0 | 1 | 0 | 0 | 0 | 0 | 0 | 0 | 0 | 0 | 0 | 0 |
| REH 2/32 | 1 | 0 | 20 | 10 | 0 | 1 | 2 | 0 | 0 | 0 | 16 | 9 | 0 |
| RKG-06 | 2 | 0 | 140 | 5 | 46 | 0 | 0 | 0 | 0 | 21 | 132 | 90 | 16 |
| RKG-07 | 4 | 0 | 4 | 5 | 3 | 2 | 3 | 0 | 1 | 0 | 3 | 4 | 0 |
| RKG-08 | 1 | 15 | 277 | 117 | 20 | 36 | 24 | 0 | 3 | 13 | 189 | 81 | 0 |
| RKG-09 | 4096 | 0 | 19 | 7 | 5 | 9 | 7 | 0 | 63 | 4 | 105 | 13 | 0 |
| RKG-10 | 2048 | 11 | 41 | 10 | 7 | 25 | 44 | 0 | 36 | 9 | 76 | 21 | 0 |
| RKG-11 | 4096 | 3 | 47 | 10 | 5 | 24 | 72 | 0 | 41 | 13 | 124 | 22 | 0 |

**A: Fraction >0.250 mm**

| Sample | Split | *Ammobaculites spp.* | *A. cretaceus* | *A. sphaeroidiniformis* | *Bathysiphon spp.* | *Bolivina spp.* | *Dentalina spp.* | *Gavelinella/Berthelina spp.* | *Gyroidinoides spp.* | *Haplophragmium sp.* | *Haplophragmoides spp.* | *Lenticulina spp.* | *M. oxycona* | *Nodosaria spp.* | *Osangularia spp.* | *Planularia spp.* | *Planulina spp.* | *P. pinawangensis* | *P. serpuloides* | *Pullenia spp.* | *Ramulina aculeata* | *Recurvoides spp.* | *Reophax spp.* | *Rotalia polyrraphes* | *Saccammina spp.* | *Spiroplectammina spp.* | *Tritaxia gaultina* | *Trochammina spp.* | *Trochamminoides spp.* | *V. münsteri* |
|---|---|---|---|---|---|---|---|---|---|---|---|---|---|---|---|---|---|---|---|---|---|---|---|---|---|---|---|---|---|---|
| RKG-01 | 128 | 0 | 0 | 0 | 0 | 0 | 0 | 0 | 0 | 0 | 1 | 0 | 0 | 0 | 0 | 0 | 0 | 0 | 0 | 0 | 0 | 0 | 1 | 0 | 1 | 0 | 0 | 0 | 0 | 1 |
| RKG-02 | 64 | 1 | 0 | 1 | 0 | 0 | 0 | 1 | 0 | 0 | 4 | 1 | 0 | 0 | 2 | 2 | 0 | 0 | 0 | 0 | 0 | 0 | 0 | 0 | 0 | 0 | 0 | 0 | 0 | 1 |
| RKG-12 | 64 | 0 | 1 | 0 | 0 | 0 | 0 | 0 | 0 | 0 | 0 | 1 | 1 | 1 | 0 | 0 | 0 | 0 | 0 | 0 | 0 | 0 | 0 | 0 | 0 | 0 | 0 | 2 | 0 | 0 |
| RKG-03 | 128 | 0 | 1 | 0 | 1 | 0 | 0 | 0 | 0 | 0 | 0 | 0 | 1 | 0 | 0 | 0 | 0 | 0 | 2 | 1 | 0 | 0 | 0 | 1 | 0 | 0 | 3 | 0 | 1 | 0 |
| REH4/4u | 128 | 0 | 0 | 0 | 0 | 0 | 0 | 0 | 2 | 0 | 0 | 0 | 0 | 0 | 2 | 0 | 0 | 0 | 0 | 0 | 0 | 0 | 0 | 0 | 0 | 0 | 3 | 0 | 0 | 0 |
| REH4/4o | 32 | 0 | 0 | 0 | 0 | 0 | 0 | 0 | 0 | 0 | 0 | 1 | 0 | 0 | 0 | 0 | 2 | 0 | 0 | 0 | 0 | 0 | 0 | 1 | 1 | 1 | 1 | 0 | 0 | 0 |
| REH4/2B | 64 | 1 | 0 | 1 | 0 | 0 | 0 | 0 | 0 | 0 | 0 | 1 | 0 | 0 | 0 | 0 | 0 | 0 | 0 | 0 | 0 | 0 | 0 | 0 | 1 | 2 | 1 | 1 | 0 | 0 |
| RKG-04 | 128 | 0 | 0 | 0 | 0 | 1 | 0 | 0 | 0 | 0 | 0 | 0 | 0 | 0 | 0 | 0 | 0 | 1 | 0 | 0 | 0 | 0 | 0 | 0 | 1 | 0 | 0 | 0 | 0 | 1 |
| RKG-05 | 64 | 0 | 0 | 0 | 1 | 0 | 0 | 0 | 1 | 0 | 0 | 0 | 0 | 0 | 0 | 1 | 0 | 0 | 0 | 0 | 0 | 0 | 0 | 2 | 0 | 0 | 0 | 0 | 0 | 0 |
| RKG-14 | 32 | 0 | 0 | 1 | 0 | 0 | 0 | 1 | 0 | 0 | 0 | 0 | 0 | 0 | 0 | 0 | 0 | 0 | 0 | 0 | 0 | 1 | 0 | 0 | 0 | 0 | 0 | 0 | 0 | 0 |
| *REH4/1* | *1* | *0* | *0* | *0* | *0* | *0* | *0* | *0* | *0* | *0* | *0* | *0* | *0* | *0* | *0* | *0* | *2* | *0* | *1* | *0* | *0* | *0* | *0* | *0* | *0* | *0* | *0* | *0* | *0* | *0* |
| RKG-15 | 1 | 0 | 0 | 0 | 0 | 0 | 0 | 0 | 0 | 0 | 0 | 0 | 0 | 0 | 0 | 0 | 0 | 0 | 0 | 0 | 0 | 0 | 0 | 0 | 0 | 0 | 0 | 0 | 0 | 0 |
| REH2/31 | 8 | 0 | 0 | 0 | 0 | 0 | 0 | 0 | 0 | 0 | 0 | 0 | 0 | 0 | 0 | 0 | 0 | 0 | 0 | 0 | 0 | 0 | 0 | 0 | 0 | 0 | 0 | 0 | 0 | 0 |
| REH2/32 | 1 | 0 | 0 | 0 | 0 | 0 | 0 | 0 | 0 | 0 | 0 | 0 | 0 | 0 | 0 | 0 | 0 | 0 | 0 | 0 | 0 | 0 | 0 | 0 | 0 | 0 | 0 | 0 | 0 | 0 |
| RKG-06 | 1 | 0 | 0 | 0 | 0 | 0 | 0 | 0 | 0 | 0 | 0 | 0 | 0 | 0 | 0 | 0 | 0 | 0 | 0 | 0 | 0 | 0 | 0 | 0 | 0 | 0 | 0 | 0 | 0 | 0 |
| RKG-07 | 1 | 0 | 0 | 0 | 0 | 0 | 0 | 0 | 0 | 0 | 0 | 0 | 0 | 0 | 0 | 0 | 0 | 0 | 0 | 0 | 0 | 0 | 0 | 0 | 0 | 0 | 0 | 0 | 0 | 0 |
| RKG-08 | 1 | 0 | 0 | 1 | 0 | 0 | 0 | 0 | 0 | 0 | 0 | 0 | 0 | 0 | 0 | 0 | 0 | 0 | 0 | 0 | 0 | 0 | 0 | 0 | 0 | 0 | 0 | 0 | 0 | 0 |
| RKG-09 | 512 | 0 | 0 | 0 | 0 | 0 | 0 | 0 | 0 | 0 | 1 | 0 | 0 | 0 | 0 | 1 | 0 | 0 | 0 | 0 | 0 | 0 | 0 | 1 | 0 | 0 | 0 | 0 | 0 | 0 |
| RKG-10 | 128 | 0 | 0 | 0 | 0 | 0 | 0 | 0 | 0 | 0 | 0 | 0 | 0 | 0 | 0 | 0 | 0 | 0 | 0 | 0 | 0 | 0 | 0 | 0 | 0 | 0 | 0 | 0 | 0 | 0 |
| RKG-11 | 256 | 1 | 0 | 0 | 0 | 0 | 1 | 0 | 0 | 0 | 0 | 0 | 0 | 0 | 0 | 0 | 0 | 0 | 0 | 0 | 0 | 0 | 0 | 0 | 0 | 0 | 0 | 0 | 0 | 0 |

**B: Fraction 0.125-0.250 mm**

| Sample | Split | *Ammobaculites spp.* | *A. mosbyensis* | *A. karrygerae* | *A. sphaeroidiniformis* | *Bathysiphon spp.* | *Bolivina spp.* | *C. beaumontianus* | *Dentalina spp.* | *Eouvigerina spp.* | *Gavelinella/Berthelina spp.* | *Gyroidinoides spp.* | *Haplophragmoides spp.* | *H. gaultina* | *Kalamopsis spp.* | *Lenticulina spp.* | *M. oxycona* | *Martinottiella spp.* | *N. albertensis* | *Nodosaria spp.* | *N. cf. robusta* | *Osangularia spp.* | *Planularia spp.* | *Planulina spp.* | *P. subnodosa* | *Praebulimina spp.* | *P. fusca* | *Pullenia spp.* | *Recurvoides spp.* | *Reophax spp.* | *R. indivisa* | *R. polyrraphes* | *Saccammina spp.* | *Spiroplectammina spp.* | *T. gaultina* | *Trochammina spp.* | *Trochamminoides spp.* | unknown calcareous foraminifera | *V. münsteri* | *Wheelerella sp.* |
|---|---|---|---|---|---|---|---|---|---|---|---|---|---|---|---|---|---|---|---|---|---|---|---|---|---|---|---|---|---|---|---|---|---|---|---|---|---|---|---|
| RKG-01 | 1024 | 0 | 0 | 0 | 0 | 0 | 0 | 0 | 0 | 0 | 4 | 5 | 0 | 0 | 0 | 0 | 0 | 0 | 0 | 0 | 0 | 4 | 0 | 0 | 0 | 0 | 0 | 0 | 0 | 0 | 0 | 0 | 0 | 0 | 0 | 0 | 0 | 0 | 0 | 0 |
| RKG-02 | 1024 | 0 | 0 | 0 | 0 | 0 | 2 | 0 | 0 | 0 | 6 | 1 | 1 | 0 | 0 | 0 | 0 | 0 | 0 | 0 | 0 | 1 | 1 | 0 | 0 | 1 | 0 | 0 | 0 | 0 | 0 | 0 | 0 | 3 | 0 | 0 | 0 | 0 | 0 | 0 |
| RKG-12 | 512 | 0 | 0 | 0 | 0 | 0 | 0 | 0 | 0 | 0 | 16 | 11 | 0 | 0 | 2 | 0 | 0 | 1 | 0 | 0 | 0 | 0 | 1 | 0 | 2 | 0 | 1 | 0 | 0 | 0 | 0 | 0 | 0 | 3 | 0 | 0 | 0 | 0 | 0 | 0 |
| RKG-03 | 1024 | 1 | 0 | 0 | 0 | 5 | 0 | 0 | 0 | 0 | 0 | 3 | 0 | 0 | 0 | 0 | 0 | 0 | 0 | 0 | 0 | 1 | 0 | 0 | 0 | 0 | 0 | 0 | 1 | 0 | 1 | 3 | 1 | 0 | 0 | 0 | 1 | 2 | 0 | 0 |
| REH4/4u | 1024 | 1 | 0 | 0 | 0 | 0 | 0 | 0 | 0 | 0 | 1 | 0 | 0 | 0 | 0 | 0 | 0 | 0 | 0 | 0 | 0 | 1 | 0 | 0 | 0 | 0 | 0 | 0 | 0 | 0 | 1 | 0 | 0 | 0 | 0 | 0 | 0 | 1 | 0 | 0 |
| REH4/4o | 256 | 0 | 0 | 0 | 0 | 0 | 0 | 0 | 0 | 0 | 1 | 1 | 0 | 0 | 0 | 0 | 0 | 0 | 0 | 0 | 0 | 1 | 0 | 0 | 0 | 0 | 1 | 0 | 0 | 0 | 0 | 0 | 0 | 0 | 0 | 0 | 0 | 1 | 0 | 0 |
| REH4/2B | 512 | 1 | 0 | 0 | 0 | 2 | 1 | 0 | 2 | 0 | 1 | 3 | 0 | 0 | 0 | 1 | 0 | 0 | 0 | 0 | 0 | 1 | 1 | 0 | 0 | 0 | 0 | 0 | 0 | 0 | 0 | 0 | 0 | 0 | 0 | 0 | 0 | 0 | 0 | 0 |
| RKG-04 | 1024 | 3 | 1 | 0 | 0 | 1 | 0 | 0 | 1 | 0 | 1 | 0 | 0 | 0 | 0 | 0 | 0 | 0 | 0 | 0 | 0 | 0 | 0 | 0 | 0 | 0 | 0 | 1 | 0 | 2 | 0 | 0 | 0 | 0 | 0 | 0 | 0 | 0 | 0 | 0 |
| RKG-05 | 512 | 2 | 0 | 0 | 1 | 0 | 0 | 0 | 1 | 1 | 3 | 3 | 1 | 0 | 0 | 1 | 0 | 0 | 0 | 0 | 0 | 0 | 0 | 0 | 0 | 0 | 0 | 1 | 0 | 0 | 1 | 0 | 0 | 0 | 0 | 0 | 0 | 0 | 0 | 0 |
| RKG-14 | 512 | 0 | 0 | 0 | 1 | 0 | 1 | 0 | 1 | 1 | 1 | 4 | 0 | 0 | 0 | 2 | 0 | 0 | 0 | 0 | 0 | 1 | 1 | 1 | 0 | 2 | 0 | 0 | 0 | 0 | 0 | 0 | 0 | 0 | 0 | 0 | 0 | 0 | 0 | 0 |
| *REH4/1* | *8* | *0* | *0* | *0* | *0* | *0* | *0* | *0* | *0* | *0* | *2* | *0* | *1* | *0* | *0* | *0* | *0* | *0* | *0* | *0* | *0* | *0* | *0* | *0* | *0* | *0* | *0* | *0* | *0* | *0* | *0* | *0* | *0* | *0* | *0* | *0* | *0* | *0* | *1* | *0* |
| RKG-15 | 32 | 0 | 0 | 0 | 0 | 0 | 0 | 0 | 0 | 0 | 0 | 0 | 2 | 0 | 0 | 0 | 0 | 0 | 0 | 0 | 0 | 0 | 0 | 0 | 0 | 0 | 0 | 0 | 0 | 0 | 0 | 0 | 0 | 0 | 0 | 0 | 0 | 0 | 0 | 0 |
| REH2/31 | 128 | 0 | 0 | 0 | 0 | 0 | 0 | 0 | 0 | 0 | 0 | 0 | 0 | 0 | 0 | 0 | 0 | 0 | 0 | 0 | 0 | 0 | 0 | 0 | 0 | 0 | 0 | 0 | 0 | 0 | 0 | 0 | 0 | 0 | 0 | 0 | 0 | 0 | 0 | 0 |
| REH2/32 | 1 | 0 | 0 | 0 | 0 | 0 | 0 | 0 | 0 | 0 | 0 | 0 | 0 | 0 | 0 | 0 | 0 | 0 | 0 | 0 | 0 | 2 | 0 | 0 | 1 | 0 | 0 | 1 | 0 | 4 | 0 | 0 | 0 | 0 | 0 | 0 | 0 | 0 | 0 | 0 |
| RKG-06 | 2 | 1 | 0 | 0 | 0 | 0 | 1 | 1 | 2 | 0 | 4 | 4 | 1 | 1 | 0 | 1 | 0 | 0 | 0 | 0 | 0 | 0 | 0 | 0 | 6 | 0 | 0 | 0 | 1 | 0 | 0 | 0 | 0 | 0 | 0 | 0 | 0 | 0 | 0 | 0 |
| RKG-07 | 2 | 5 | 0 | 0 | 0 | 3 | 0 | 0 | 0 | 0 | 0 | 0 | 1 | 0 | 0 | 0 | 0 | 0 | 0 | 0 | 0 | 0 | 0 | 0 | 0 | 0 | 0 | 0 | 0 | 6 | 0 | 0 | 0 | 0 | 0 | 0 | 0 | 0 | 0 | 0 |
| RKG-08 | 1 | 1 | 0 | 1 | 0 | 0 | 0 | 0 | 0 | 0 | 0 | 1 | 0 | 0 | 0 | 1 | 0 | 0 | 0 | 0 | 1 | 0 | 0 | 0 | 1 | 0 | 0 | 0 | 0 | 2 | 0 | 0 | 0 | 0 | 0 | 0 | 0 | 4 | 0 | 0 |
| RKG-09 | 4096 | 0 | 0 | 0 | 0 | 0 | 0 | 0 | 0 | 0 | 1 | 3 | 0 | 0 | 0 | 0 | 0 | 0 | 0 | 0 | 0 | 0 | 1 | 0 | 0 | 2 | 0 | 0 | 0 | 4 | 0 | 0 | 0 | 0 | 0 | 0 | 0 | 6 | 0 | 0 |
| RKG-10 | 1024 | 2 | 0 | 0 | 0 | 0 | 0 | 0 | 0 | 0 | 4 | 0 | 3 | 0 | 0 | 0 | 0 | 0 | 0 | 0 | 0 | 3 | 0 | 0 | 3 | 0 | 0 | 0 | 0 | 1 | 0 | 0 | 0 | 0 | 0 | 0 | 0 | 0 | 0 | 0 |
| RKG-11 | 2048 | 0 | 0 | 0 | 0 | 0 | 0 | 0 | 0 | 0 | 0 | 0 | 0 | 0 | 0 | 0 | 0 | 0 | 0 | 0 | 0 | 0 | 0 | 0 | 1 | 0 | 3 | 0 | 0 | 3 | 0 | 0 | 0 | 0 | 0 | 0 | 0 | 0 | 0 | 0 |

**C: Fraction 0.063-0.125 mm**

| Sample | Split | *Ammobaculites spp.* | *A. sphaeroidiniformis* | *Bathysiphon spp.* | *Bolivina spp.* | *Dentalina spp.* | *Eouvigerina spp.* | *G. cf. ogugensis* | *Gavelinella/Berthelina spp.* | *Gyroidinoides spp.* | *Haplophragmoides spp.* | *Lenticulina spp.* | *N. albertensis* | *Nodosaria spp.* | *Nonionella cf. robusta* | *Osangularia spp.* | *Planularia spp.* | *Planulina spp.* | *Praebulimina spp.* | *Pullenia spp.* | *Recurvoides spp.* | *Reophax spp.* | *R. indivisa* | *Saccammina spp.* | *Schellnerova spp.* | *Spiroplectammina spp.* | *T. lachiosa* | *Trochammina spp.* | *Trochamminoides spp.* | unknown calcareous foraminifera |
|---|---|---|---|---|---|---|---|---|---|---|---|---|---|---|---|---|---|---|---|---|---|---|---|---|---|---|---|---|---|---|
| RKG-01 | 16384 | 1 | 0 | 0 | 0 | 0 | 0 | 5 | 28 | 2 | 1 | 0 | 4 | 0 | 0 | 2 | 0 | 4 | 7 | 1 | 0 | 2 | 0 | 0 | 0 | 0 | 0 | 0 | 0 | 0 |
| RKG-02 | 8192 | 7 | 0 | 1 | 0 | 1 | 0 | 14 | 2 | 6 | 4 | 0 | 21 | 0 | 0 | 6 | 0 | 4 | 8 | 0 | 0 | 2 | 0 | 0 | 0 | 0 | 0 | 0 | 0 | 0 |
| RKG-12 | 8192 | 0 | 0 | 0 | 0 | 0 | 0 | 2 | 7 | 7 | 0 | 0 | 2 | 0 | 0 | 0 | 0 | 2 | 24 | 0 | 0 | 0 | 0 | 0 | 0 | 0 | 0 | 1 | 0 | 1 |
| RKG-03 | 8192 | 1 | 0 | 0 | 0 | 2 | 0 | 1 | 3 | 5 | 0 | 0 | 2 | 0 | 0 | 0 | 0 | 1 | 4 | 1 | 0 | 0 | 0 | 0 | 2 | 0 | 0 | 0 | 0 | 0 |
| REH4/4u | 8192 | 0 | 0 | 1 | 0 | 1 | 0 | 3 | 0 | 5 | 0 | 0 | 5 | 1 | 0 | 0 | 0 | 0 | 4 | 0 | 0 | 2 | 0 | 0 | 0 | 0 | 0 | 0 | 0 | 0 |
| REH4/4o | 2048 | 0 | 0 | 1 | 1 | 1 | 0 | 0 | 3 | 3 | 0 | 0 | 2 | 0 | 1 | 2 | 0 | 1 | 7 | 0 | 1 | 0 | 0 | 0 | 0 | 0 | 0 | 0 | 0 | 0 |
| REH4/2B | 4096 | 4 | 0 | 0 | 0 | 0 | 0 | 0 | 0 | 3 | 0 | 0 | 2 | 0 | 0 | 0 | 0 | 1 | 5 | 1 | 0 | 0 | 0 | 0 | 0 | 0 | 0 | 0 | 0 | 0 |
| RKG-04 | 8192 | 0 | 0 | 0 | 0 | 0 | 0 | 0 | 0 | 5 | 0 | 0 | 2 | 0 | 0 | 0 | 0 | 0 | 18 | 0 | 0 | 0 | 0 | 0 | 0 | 0 | 0 | 0 | 0 | 0 |
| RKG-05 | 4096 | 3 | 0 | 2 | 0 | 0 | 0 | 0 | 2 | 5 | 0 | 0 | 6 | 0 | 0 | 1 | 0 | 0 | 25 | 0 | 0 | 0 | 0 | 0 | 0 | 0 | 0 | 0 | 0 | 0 |
| RKG-14 | 4096 | 0 | 0 | 4 | 4 | 0 | 0 | 0 | 8 | 13 | 0 | 0 | 6 | 0 | 0 | 0 | 0 | 1 | 25 | 0 | 0 | 0 | 0 | 0 | 5 | 0 | 0 | 0 | 0 | 0 |
| *REH4/1* | *64* | *0* | *0* | *0* | *0* | *0* | *1* | *0* | *1* | *1* | *0* | *0* | *2* | *0* | *0* | *0* | *0* | *0* | *0* | *0* | *0* | *0* | *1* | *0* | *0* | *0* | *0* | *0* | *0* | *0* |
| RKG-15 | 64 | 0 | 2 | 0 | 4 | 0 | 0 | 0 | 0 | 0 | 4 | 0 | 0 | 0 | 0 | 0 | 0 | 0 | 0 | 0 | 0 | 0 | 0 | 0 | 1 | 0 | 0 | 2 | 0 | 0 |
| REH2/31 | 256 | 0 | 0 | 0 | 0 | 0 | 0 | 0 | 0 | 0 | 0 | 0 | 0 | 0 | 2 | 0 | 0 | 0 | 0 | 0 | 0 | 0 | 0 | 0 | 0 | 0 | 0 | 0 | 0 | 0 |
| REH2/32 | 1 | 8 | 0 | 2 | 1 | 0 | 0 | 0 | 4 | 0 | 0 | 0 | 0 | 0 | 0 | 2 | 0 | 2 | 1 | 3 | 0 | 1 | 0 | 0 | 0 | 0 | 0 | 0 | 0 | 2 |
| RKG-06 | 2 | 1 | 0 | 0 | 0 | 2 | 2 | 0 | 0 | 5 | 1 | 1 | 0 | 0 | 0 | 0 | 0 | 2 | 0 | 2 | 2 | 0 | 0 | 0 | 0 | 0 | 0 | 0 | 0 | 0 |
| RKG-07 | 4 | 8 | 0 | 5 | 1 | 0 | 3 | 0 | 0 | 9 | 0 | 1 | 5 | 0 | 0 | 0 | 0 | 1 | 4 | 0 | 0 | 9 | 0 | 0 | 0 | 0 | 0 | 0 | 0 | 0 |
| RKG-08 | 1 | 3 | 0 | 0 | 1 | 0 | 0 | 0 | 0 | 13 | 0 | 0 | 1 | 0 | 0 | 0 | 0 | 0 | 27 | 0 | 0 | 4 | 0 | 0 | 0 | 0 | 0 | 0 | 0 | 1 |
| RKG-09 | 4096 | 4 | 0 | 0 | 0 | 0 | 1 | 4 | 0 | 5 | 0 | 0 | 5 | 0 | 0 | 0 | 0 | 7 | 8 | 0 | 0 | 7 | 0 | 0 | 0 | 0 | 0 | 0 | 0 | 0 |
| RKG-10 | 2048 | 4 | 0 | 0 | 0 | 0 | 0 | 0 | 4 | 9 | 1 | 0 | 5 | 1 | 0 | 0 | 0 | 0 | 12 | 0 | 0 | 12 | 0 | 0 | 0 | 0 | 0 | 0 | 0 | 2 |
| RKG-11 | 4096 | 0 | 0 | 0 | 0 | 0 | 0 | 0 | 0 | 3 | 0 | 0 | 3 | 0 | 0 | 0 | 0 | 4 | 26 | 0 | 0 | 9 | 0 | 0 | 0 | 0 | 0 | 4 | 1 | 0 |

| | Fraction >0.250 mm | | Fraction 0.125-0.250 mm | | Fraction 0.063-0.125 mm | |
|---|---|---|---|---|---|---|
| **sample** | **split** | **no.** | **split** | **no.** | **split** | **no.** |
| RKG-01 | 32 | 0 | 32 | 67 | 512 | 90 |
| RKG-02 | 16 | 10 | 32 | 195 | 512 | 85 |
| RKG-12 | 32 | 0 | 64 | 55 | 1024 | 16 |
| RKG-03 | 32 | 1 | 64 | 55 | 1024 | 15 |
| REH 4/4 u | 32 | 0 | 64 | 66 | 512 | 32 |
| REH 4/4 o | 16 | 0 | 32 | 51 | 128 | 25 |
| REH 4/2b | 16 | 0 | 32 | 40 | 256 | 17 |
| RKG-04 | 16 | 0 | 64 | 45 | 512 | 30 |
| RKG-05 | 16 | 2 | 32 | 85 | 256 | 35 |
| RKG-14 | 16 | 9 | 64 | 86 | 512 | 60 |
| RKG-15 | 4 | 94 | 64 | 113 | 16 | 28 |
| REH 2/31 | 16 | 105 | 256 | 31 | 256 | 4 |
| REH 2/32 | 2 | 5 | 4 | 124 | 16 | 44 |
| RKG-06 | 1 | 303 | 16 | 304 | 8 | 117 |
| RKG-07 | 1 | 99 | 32 | 188 | 64 | 108 |
| RKG-08a | 1 | 2 | 8 | 0 | 2 | 11 |
| RKG-09 | 32 | 1 | 512 | 52 | 1024 | 33 |
| RKG-10 | 32 | 0 | 128 | 16 | 256 | 44 |
| RKG-11 | 32 | 2 | 256 | 38 | 512 | 50 |

| Sample | Lithology | δ13Corg | Dry sample weight [g] | Planktic foraminifera [ind/gr] | Radiolaria [ind/gr] | Radiolaria/ planktic foraminifera ratio | Benthic foraminifera [ind/gr] |
|---|---|---|---|---|---|---|---|
| RKG-01 | marl | -25,38 | 129 | 53807,63 | 373,83 | 0,007 | 7402,17 |
| RKG-02 | marl | -25,92 | 132 | 32784,48 | 378,18 | 0,012 | 4847,03 |
| RKG-12 | marl | -25,95 | 176 | 22314,55 | 113,09 | 0,005 | 2242,55 |
| RKG-03 | marl | -25,02 | 218 | 11495,34 | 86,75 | 0,008 | 917,72 |
| REH 4/4 u | calcareous marl | n.d. | 191 | 24698,64 | 107,90 | 0,004 | 969,05 |
| REH 4/4 o | marl | n.d. | 36 | 25163,56 | 134,22 | 0,005 | 1350,22 |
| REH 4/2b | marl | n.d. | 106 | 17552,30 | 53,13 | 0,003 | 685,89 |
| RKG-04 | marl | -25,64 | 175 | 19167,82 | 104,23 | 0,005 | 1231,73 |
| RKG-05 | marl | -24,89 | 69 | 17997,91 | 169,74 | 0,009 | 2743,65 |
| REH02/30B1 | limestone | -26,10 | n.d. | n.d. | n.d. | n.d. | n.d. |
| REH02/30B2 | limestone | -25,94 | n.d. | n.d. | n.d. | n.d. | n.d. |
| RKG-14 | calcareous marl | -25,12 | 86 | 22000,00 | 422,88 | 0,019 | 3258,05 |
| *REH 4/1* | clay | n.d. | *63* | n.d. | n.d. | n.d. | n.d. |
| RKG-15 | black shale | -24,01 | 61,2 | 2,14 | 131,63 | 61,496 | 14,64 |
| REH02/31m | black shale | -23,80 | n.d. | n.d. | n.d. | n.d. | n.d. |
| REH 2/31o | black shale | -23,30 | 199 | 1,29 | 53,47 | 41,563 | 2,57 |
| REH 2/32 | clayey marl | -24,11 | 95 | 0,83 | 12,74 | 15,316 | 0,37 |
| RKG-06 | black shale | -24,65 | 147 | 10,61 | 41,52 | 3,912 | 0,61 |
| RKG-07 | clayey marl | -24,65 | 257 | 0,50 | 50,69 | 101,773 | 0,86 |
| REH02/34C | claystone | -26,09 | n.d. | n.d. | n.d. | n.d. | n.d. |
| RKG-08 | marl | n.d. | 110 | 10,74 | 0,22 | 0,020 | 0,59 |
| RKG-09 | marl | -25,77 | 662 | 4174,89 | 91,31 | 0,022 | 361,18 |
| RKG-10 | marl | -28,73 | 85 | 12584,66 | 156,61 | 0,012 | 1421,55 |
| RKG-11 | marl | -28,08 | 214 | 12366,95 | 165,38 | 0,013 | 1055,10 |

n.d. = not determined